

Dear Editor!

We thank the reviewers for taking the time (clearly more than just a day) to carefully read the manuscript, to think about the contents, and then to come up with a constructive, fruitful list of suggestions that now, hopefully, lead to a significantly improvement of the revised version.

Some general remarks, first: We changed the contents considerably according to the reviewers' suggestions, but also by re-thinking the entire concept, methodology, and discussion of the two observational cases.

(1) In the introduction, we extended the discussion regarding the potential problems introduced by the use of a spheroidal particle shape model when applied to LIRIC, or more general, to lidar observations, i.e., in cases where the retrievals are based on aerosol scattering at exactly  $180^\circ$ .

(1) The methodology is re-written, to include, right from the beginning, the fact that a cross-polarized backscatter signal is measured. This is now considered in the formulas by using an index  $p$  indicating the polarization state.

(2) We re-checked all figures and had to replace some. As a new point, now we show in Figures 4, 5, 10, and 11 besides the POLIPHON results for spherical and non-spherical particle fractions and LIRIC results for fine-mode and coarse-mode particles (as in the submitted version), LIRIC results for spherical and non-spherical particles. In this way a direct comparison of POLIPHON and LIRIC results is possible. This work took time (some weeks), new computations were necessary.

(3) Figure 6 now only shows lidar ratio and depolarization ratio values, and a new Figure 7 is added and shows the Angstrom exponents (for backscatter, extinction, lidar ratio). With Figure 7 we clearly show now the impact of the spheroidal model on the LIRIC retrieval results. The spheroidal particle model introduces significant uncertainty. This was already the message of several papers as Mueller et al., 2010, 2012, and Gasteiger et al. 2011. Now our results in Figures 6 and 7 corroborate these findings. The results in Figs. 6 and 7 are in full agreement with the literature so that there is no doubt left that the spheroidal model is the main error source here for the observed discrepancies.

Similarly, for the volcanic case, Figure 12 now shows lidar ratio and depolarization ratio profiles only. A new Figure 13 shows the backscatter-related, extinction-related, and lidar-ratio-related Angstrom exponents. In Figure 13, the agreement between LIRIC results and direct Raman lidar observations is worse and the reason is most probably the observed complex aerosol mixing and layering so that the simple use of height-independent volume-specific backscatter and extinction coefficients required in LIRIC and delivered by AERONET leads to large uncertainties.

(4) We extended the error discussion and include now overlap correction uncertainties, uncertainties introduced by varying minimum and maximum measurement heights, and uncertainties in the estimate of the reference particle backscatter value at the reference height.

Based on this new set of Figures we extended the discussion (in the result section), rechecked our explanations, and improved the discussion along the lines suggested by the reviewers.

-----  
Anonymous Referee #1

The description of the method is clear and thorough (a more extended description would be out of the scope of the paper).

**Yes, we agree, we should not extend the description here.**

LIRIC-retrieved particle concentrations are evaluated using the corresponding concentrations retrieved with the POLIPHON method. As seen in the text, this comparison is problematic, since the definition of fine and coarse modes is different for the two methods. Although some insight is given through the comparison of retrieved backscatter coefficient profiles for fine and coarse modes, the comparison deems inconclusive, especially for the mixed case. In addition, POLIPHON and LIRIC uncertainties are not explicitly quantified. A further investigation of these uncertainties (by varying the minimum and reference heights, changing the overlap correction but also by taking into account the uncertainty in the density value used for the conversion from volume to mass concentration) would make this work more complete, but it is not mandatory. Irrespectively, an overall evaluation of the comparison of LIRIC and POLIPHON results, summarizing the assumptions of each method and including a discussion of the problems in error estimation, would be very clarifying and is necessary in the conclusions section.

**Keeping these comments in mind we checked the errors occurring when varying minimum and reference height and by using different overlap functions. We quantified the uncertainties and mention them in the text (section 4, for both observational cases). We furthermore introduce a Table 1 with all the essential assumptions used in the LIRIC and POLIPHON procedures. We discuss all the additional uncertainties (by overlap correction, by minimum and maximum height variations) not covered by the error bars. However, we leave out to discuss the uncertainties in the POLIPHON retrieval (we show the error bars and mention the main error sources, and show the input parameters in Table 1) . This is enough here. This is a LIRIC paper, not a POLIPHON paper. Ansmann et al. (2012) discuss the POLIPHON errors.**

Also, please provide in the conclusions section other methods that would be more appropriate to use for LIRIC validation (e.g. using airborne in-situ data?)

**We suggest airborne in-situ data for validation..., but our experience with SAMUM (airborne Saharan dust observations) and aircraft overflights over the Leipzig lidar after the Eyjafjallajökull volcanic eruptions let us believe that the uncertainties in the aircraft data are even larger than the ones in our remote sensing products (because of inlet problems, furthermore by using optical methods to get the size distribution, but the particles are non spherical!!!, and the refractive index must be assumed too..., and so on).**

Page 913

1-10 “The recently. . . radius range from 0.194  $\mu\text{m}$ -0.576  $\mu\text{m}$ .”: Needs rephrasing, e.g.: “The recently developed Lidar/Radiometer Inversion Code (LIRIC) was designed as a universal code for processing lidar/photometer network data, applicable to many different instrumental conditions and technical approaches. LIRIC uses the profiles of elastic-backscatter signals measured with multi-wavelength lidar and the spectrally-resolved column-integrated particle optical properties from photometer

observations in a synergistic way (Chaikovsky et al., 2008, 2012). The main purpose is the retrieval of height distributions of optical and microphysical properties of fine-mode and coarse-mode particles. In accordance to the AERONET data analysis code, the method searches for the minimum in the bimodal particle volume size distribution in the particle radius range from 0.194  $\mu\text{m}$ -0.576  $\mu\text{m}$ .”

**Done!**

11-13 “In this contribution. . . irregularly shaped dust particles.”: The validation of LIRIC is done using POLIPHON results which though contain uncertainties as well, especially for mixed cases. It is better to rephrase this piece to reflect the validation method uncertainty.

**Yes, the POLIPHON uncertainties are now mentioned in the introduction section, and later on several times.**

16 “The inversion. . . to obtain. . .”: Change to “The inversion of AERONET sky radiance measurements to obtain. . .”

**Done!**

23 “The method”: Change to “LIRIC method”

**Done!**

18-22 “These overlap. . . heights of 150 m”: The overlap correction is associated with an uncertainty. Has this uncertainty been quantified and taken into account in the estimation of the signal dispersion at the later steps of the analysis (page 926 lines 7-8 “The incomplete overlap. . . height.”, page 931 lines 22-25 “Part of the systematic. . . overlap correction.” and page 932 lines 20-22 “In the case. . . with decreasing height”)? Please discuss.

**We discuss the overlap correction uncertainty now in detail, and we quantify the errors for different height ranges now in section 4.1 (Saharan dust case) and again in section 4.2 (volcanic case).**

24 “Sun-sky photometers applied by AERONET”: Change to “AERONET sun-sky photometers”

**Done!**

28 “Sky radiance observations”: Change to “Sun and sky radiance observations” (see Dubovik and King, 2000).

**Done!**

Page 916

4-5 “Based on these microphysical properties, AERONET provides the optical characteristics (the AOT, the column volume concentrations. . .”: The AOT is not retrieved, it is measured. The volume concentrations are not optical properties. Rephrase accordingly. 7-9 “In a case when sky radiance observations are not available the AOT and the column volume concentrations are derived from spectral dependence. . .”: Change to “For cases when sky radiance observations are not available the AOT and the column volume concentrations are derived from the spectral dependence. . .”

**Done!**

Page 917

1 “RFOV”: Spell out the acronym.

**Done!**

7 “. . .to increases the. . .”: Change to “. . .to increase the. . .”

**Done!**

Page 918

5-6 “In the case of 1064 nm. . . at the reference height.”: What is the estimate used in the analysis?

**We state that we use a backscatter ratio of 1.1 at the reference height for all three wavelengths.**

11-12 “To assure optimized profiles. . . within error margins.”: Provide reference on optimization method.

**We provide the reference, Eadie et al., 1971**

Page 919

4-10 For Eq. 7, 8, 9 provide explanations for symbols used (e.g.  $\omega$ , F11) immediately after. (The explanations are provided in the text, but further below.)

**Done!**

16-17 “A fixed fraction. . . for the fine mode...”: Provide the value of the ratio.

**We say that LIRIC uses the actual sphericity value determined by AERONET as input to compute the ratio of spherical to non-spherical particles.**

22-24 “Besides. . . data set.”: Make more explicit the option of including the cross-polarized 532 nm backscatter signal. Rephrase to: “Besides the elastic backscatter signals for 355, 532, and 1064 nm, LIRIC algorithm provides the option of including the cross-polarized 532 nm backscatter signal (denoted as 532c in Fig. 1, wavelength index  $j=4$ ) in the input signal data set.”

**This is now changed in a more extended way because we re-formulated the entire methodology section and consider, right from the beginning, the cross-polarized signal in the LIRIC retrieval.**

Page 920

1-2 “Consequently, . . . non-spherical particles.”: Rephrase it to highlight that if the cross-polarized signal is not provided LIRIC does not provide results for non-spherical particles.

**See statements before (full consideration of the cross-polarized signal from the beginning)...**

13-14 “The retrieval is designed. . . in Dubovik, 2004.”: (OPTIONAL) Change to: “The retrieval is designed as statistically optimized fitting of multi-source data, using the multi-term LSM (see detailed description in Dubovik, 2004).”

**We changed the text as a whole and implemented this comment.**

15 “. . .is organized as minimization. . .”: (OPTIONAL) Change to “. . .is organized as the minimization. . .”.

**Done!**

17-8 “. . .photometric measurements and retrieved concentration profiles,. . .”: Change to “. . .photometer-derived column volume concentrations and corresponding integrals of the retrieved concentration profiles,. . .”.

**Done!**

Page 921

1-2 “The mean value of the different solutions. . . 5-10 different solutions.”: Discuss why you didn’t take into account the minimum and reference height uncertainty in the error estimation.

**Done! We now extend the error discussion and mention the impact of overlap correction uncertainties and variations in the minimum and reference heights. But these are quite different error sources than the ones originating from the LIRIC procedure itself and the basic LIRIC retrieval assumptions. But as mentioned this is now explained in the text accordingly.**

Page 923

8-10 “. . .are caused by. . . related to the coarse mode.”: Rephrase “. . .are caused by non-depolarizing spherical particles (i.e. fine-mode fraction), and that the coarse mode are strongly light-depolarizing non-spherical particles.”

**Done!**

25 “. . .required. . . in addition).”: Change to “. . .required in the LIRIC data analysis).”

**Done!**

Page 925

20 “Stable conditions. . .”: Since you provide evidence for these “stable conditions” below (page 926, line 10), rephrase as “Stable conditions (see discussion below). . .”

**Done!**

23 “. . .,21:47 to 23 15 UTC. . .”: Why using such a broad time frame? Especially since after 22:45 there is an obvious change in the vertical distribution of the aloft plume (see Fig. 2). Discuss.

**The aerosol conditions were really stable, so that signal averaging is ok. Even after 23:15 the aerosol distribution did not change significantly.**

Page 926

1-2 “Figure 3. . . as retrieved with LIRIC”: (OPTIONAL) Move line 19-20 here to highlight the absence of spherical coarse mode “Figure3. . . as retrieved with LIRIC. The analysis indicated the absence of spherical coarse-mode particles throughout the troposphere.”

**Done!**

4-5 “As mentioned. . . AERONET observations.”: (OPTIONAL) Rephrase as “As mentioned, the vertically integrated fine- and coarse-mode volume concentrations must match the respective column values retrieved from AERONET observations.”

**Done!**

Page 928

6-7 “According to Fig. 5. . . AERONET column observations”: Rephrase according to the fact that the AERONET column observations are actually used in POLIPHON analysis. Thus, POLIPHON results are not as independent from the AERONET column observations as it is implied in the phrase.

**We state at several places that POLIPHON also depends on AERONET input. And we introduced the new Table.1 to make that clear to everybody.**

10-13 “The fine-mode. . . POLIPHON curve.”: If this is true, the agreement in the coarse mode should be re-evaluated under this light. Furthermore, this discrepancy may be also due to the density used for the non-spherical fraction of fine mode ( $p_2$  in Eq.11) for the conversion of LIRIC fine mode volume to mass concentration (this also applies at page 932 lines 18-19 “Regarding. . . AERONET column value.”). Did you take into account the range of possible densities in the LIRIC and POLIPHON mass concentration uncertainties? Discuss.

**The error bars include the density uncertainty, and both LIRIC and POLIPHON use the same density values. We re-analyzed the data and also compare now the sphericity value from AERONET (and thus LIRIC) and derived from POLIPHON. So we extended the discussion significantly.**

Page 930

5 “. . . transport from the west”: (OPTIONAL) Provide reference.

**Done!**

25-28 “Cumulus cloud. . . in the coarse mode.”: Then, this is probably a failure of LIRIC to retrieve the spherical coarse mode in this case. Please include in the conclusions section.

**We improved the statements. We use cloud-screened signal profiles. So there is no cloud interference in the results.**

Page 932

9-25 “As can be seen. . . acceptable.”: Provide the densities ( $p_1$  and  $p_2$ ) used.

**Done!**

Page 933

16-17 “. . .indicated a good. . . with LIRIC.”: As mentioned in the beginning of this review, please rephrase and include a discussion about the comparison of LIRIC and POLIPHON results for each case separately (emphasizing that the mixed case is more problematic), as well as the problems in error estimation for the two methods.

**We now state more clearly the difference between the two case studies (a simple aerosol scenario versus a very complex scenario), we discuss the errors in more detail, more carefully and by better separating the different cases. We include new figures with backscatter-related, extinction-related, and lidar-ratio-related Angstrom exponents to provide more inside into the limits of LIRIC. We include LIRIC results for non-spherical and spherical particles to better compare LIRIC with POLIPHON results. So the conclusions are quite clear now.**

Page 938

Fig.1 “LIRIC products (blue box). . .depolarization ratios). . .”: Provide the symbols of the properties, as seen in the figure.

**Done!**

Fig.1 –last line “. . .and respective mass concentrations  $M_f$  and  $M_c$  for fine and coarse mode.”: The mass concentrations are not “LIRIC products”.

**Improved**

Page 940

Fig.3 (OPTIONAL) Change the “Coarse mode” in legend to “Non-spherical coarse mode”. Do the same in Fig. 4, 5, 8, 9 and 10.

**Because we extended the discussion and compare POLIPHON (spherical, non-spherical), LIRIC (spherical, non-spherical), and LIRIC (fine mode, coarse mode) and show the results in four extended figures, we left out to mention non-spherical coarse mode particles here. This is no longer necessary.**

---

Anonymous Referee #3

Received and published: 18 March 2013

General Comments

This paper describes a microphysical retrieval method for a combination of ground based elastic backscatter lidar plus an AERONET sunphotometer. .... For the most part, the paper is well written and includes an appropriate amount of explanation and detail.

However, I think the manuscript should be improved in a few key areas. I believe the conclusion should be more specific about both the positive and negative results found in the study. The authors state that one of the goals of the paper is to “evaluate the potential” of the LIRIC method, so they should specify details in the conclusion about when the method is most applicable and when it is less

applicable (i.e. the two distinct case studies had different results: why?), what are the strengths and weaknesses, and (if possible) what possibilities are there for improving the method.

**We kept these suggestions in mind when we re-phrased the entire discussion section (result and conclusion sections). According to our general statements at the beginning of this reply we extended our discussion considerably and show more comparisons, more figures. Nevertheless, in cases with complex aerosol mixing and layering it is almost impossible to come up with clear conclusions (which are then free of speculation). So these conclusions are not drawn to avoid speculations. It is too early to come up with clear conclusions. Much more studies are required. This is stated in the conclusion section.**

Also, I think the data analysis and interpretation of the case studies is somewhat weak, specifically in terms of the lists of potential explanations for discrepancies between the LIRIC and Raman/POLIPHON results. Several possible explanations are listed, but without further investigation that would help to distinguish whether or how much these different explanations contribute, even in cases where it seems like follow-up would be easy.

**The discussion now provides more details, more parameters (sphericity, several Angstrom exponents) are presented and discussed. More conclusions are now drawn.**

**We compare POLIPHON (spherical, non-spherical), LIRIC (spherical, non-spherical), and LIRIC (fine mode, coarse mode) and show the results in four extended figures, as mentioned above. More cannot be done.**

On a less critical note, I think the flow of the introduction and methodology sections could be improved to make the retrieval much clearer to the reader. While almost all of the information I would want is presented somewhere in the manuscript, the introduction could provide a better foundation for understanding the methodology and results. Also in the introduction, it would be good to add a discussion about how this technique is similar to or different from other microphysical retrieval techniques, such as Veselovskii et al. (2012), Leon et al. (2003), Veselovskii et al (2002), and Mueller et al. (1999).

**This is now considered in detail as desired.**

#### Specific Comments

Introduction (also see general comment above): I think the description of the LIRIC technique could be improved, to better prepare the reader to follow the explanations and results in subsequent sections. Specifically, I think it's important to clarify (1) what the inputs are and specifically that only backscatter (not Raman extinction) lidar signals are used for the lidar part, (2) what outputs are provided, and (3) the relationship between the AERONET retrieval and the LIRIC retrieval (that is, that the AERONET retrieval is input to the LIRIC retrieval).

**This is now done in the introduction section as suggested. And we expanded the discussion on the potential error source: spheroidal particle shape model.**

Page 915, Line 3-10: It's potentially confusing at first that you are not using the Raman extinction measurement in the retrieval. Please consider adding another sentence that would explain why only

the elastic backscatter signals are used and the motivation for having a Raman lidar for this study (i.e. for the validation).

### **This is now written in section 2.1**

Page 916: Does the radiometer inversion assume a single complex refractive index for all particles in both the fine and coarse mode in the whole column? Do you have any comment about whether this is a reasonable assumption and what effect it might be expected to have? Please discuss whether there are there any other important assumptions that might affect the accuracy besides the spheroidal model, the use of column-equivalent values of some parameters and the assumption of a single refractive index?

**We present a new table (Table 1) with ALL the assumptions made, and whether the assumed parameters are height-dependent, or assumed to be equal for both modes etc. But it is not our job to provide a very detailed error analysis about the refractive index assumptions e.g. when the agreement of the results is fine (Saharan dust) or when the agreement is bad because of complex layering and badly defined conditions for LIRIC/AERONET retrievals, ....so that a study of the impact of individual errors sources, such as the refractive index uncertainties, seems to be just speculations..**

**A discussion on the impact of uncertainties caused by the use of the column-equivalent values of some of the parameters including refractive index assumptions is not given, would be too speculative. We do not have the potential to check this all in detail. But from the discussion of the second case (volcanic aerosol) it becomes clear now that LIRIC is at its limits in cases with complex and varying aerosol layering and mixing.**

Page 916, Line 7-10: Which of these two AERONET inversions were used in the case studies examined in this paper?

### **The Dubovik code**

Page 915-916, Section 2.2: Is there is a minimum AOT required (0.4?) to obtain the AERONET inversion for use with LIRIC?

**No!**

Page 918, line 9-12 and 920, lines 13-20: This couple of paragraphs is a slightly awkward compromise between too little and too much technical information. The phrases "Multi-term LSM formulation" and "LSM-based statistically optimized retrieval procedure" by themselves are not very informative. At a minimum, Least Squares Method (?) needs to be spelled out. I think a more complete description of the retrieval method would be appropriate here (or in an appendix) since the prior Chaikovsky and Wagner references are not in peer reviewed literature. If so, then I think it would be good to have the equations that define the system (the ones described on 920 as "a quadratic functional that consists of several terms"). Less important would be a description of the inversion method including the smoothness constraint. If you prefer to have just a sentence or two without much technical detail, then I think it is important to make these sentences more descriptive and understandable by someone who is not already familiar with the Dubovik retrieval. In either case, please include the full list of references right at the start of this discussion (page 918).

**We prefer to keep the discussion short. We try to provide a better description and provide more references. The paper is already very long, and a more extended description of data processing is not appropriate. This must be done by the persons who developed LIRIC (our co-authors Chaikovsky and Dubovik). These papers are in preparation to cover this (and will be part of a special issue on EARLINET in 2014).**

Page 918, line 9: Is it covariances between different heights (or range bins) that are required or covariances between different wavelengths? Without further explanation about the covariance matrices, I'm not sure this detail adds much value.

**Covariances between heights. We changed the text, accordingly.**

Page 918, line 14-15: Consider adding "also" after profiles and adding another sentence something like this: "Comparing these profiles to the lidar measurements allows us to solve for the particle volume concentrations." With no mention of the lidar, which is better suited to measure aerosol profiles, it's confusing to read that the aerosol profiles are estimated from the photometer.

**We did.**

Page 918-919: Is the LIRIC system of equations overdetermined (after the AERONET inversion step)? It seems that there are more measurements (4 lidar measurements per range bin plus column constraints) than unknowns (3 concentrations per range bin), although of course they are not orthogonal. If so, can you make any statement about whether 3 is the minimum number of lidar wavelengths needed for this retrieval? If the authors have any basis for answering this, I think there would be interest in it.

**No, we leave out such statements, in view of so many input parameters (Table 1) we do not believe it makes sense to discuss whether there are more unknowns than measurements. How to handle all the assumptions, many assumptions are profile assumptions.**

Page 920, line 4: If you say "minimized with respect to the particle volume concentrations,  $C$ " rather than just "minimized", it would be clearer.

**Done!**

Page 920, line 26-Page 921, line 2: the idea of forming the error bars from the results of multiple runs using different regularization parameters seems a bit suspect. These presumably depend on how much the regularization parameters are tweaked and therefore are not a good representation of the propagation of the input measurement errors. While there might be an argument that the errors from different runs are random within the measurement errors (I'm not sure I actually believe that), 5-10 runs does not seem like enough variation for a Monte Carlo type error bar calculation.

**As now mentioned, the 5-10 runs are done in such a way (with well selected rather than randomly chosen input parameters and related uncertainties) that the full error range caused by the LIRIC input parameters is covered, and the. Further error sources are discussed now that are more related to the signal profiles and their preparation before applying the LIRIC algorithm. This is now stated in section 4.**

Page 923, line 15: Reference the earlier work by Sugimoto et al (2003). Tesche et al. (2009) are responsible for applying the equations from Sugimoto et al. to extinction from a Raman lidar. Since you are partitioning only the backscatter, I think the prior reference is appropriate.

**Done!**

Page 923, line 23: "The parameters  $a_f$  and  $a_c$  are almost insensitive . . .". What is the basis for this statement? Please add an explanation and reference.

**As shown by Dubovik et al. (2006) the phase functions for spherical and spheroidal particles are very similar for forward scattering up to scattering angles of 20 degrees or so. And these angles are almost completely responsible for the extinction coefficient. So, the extinction coefficient is the same for spheres or spheroids, and so we conclude ... independent of shape. This is explained in the text.**

Page 924, line 9: "obtained from the Raman lidar measurements or from combined photometer-lidar observations". Which option was used for the cases presented here? If the Raman lidar ratio measurements are used, is it still a column-equivalent value, or in that case are  $S_{aer1}$  and  $S_{aer2}$  height dependent?

**No it is a column-integrated value.**

Figure 4 and discussion, Page 926, line 27. I'm confused why the LIRIC derived coarse mode backscatter coefficient is lower than POLIPHON for the peak near 2 km, but the particle depolarization ratio at that height is greater (in Figure 6). I would expect both errors in the same direction.

**The related Figures are checked and several errors are found (partly wrong profiles were calculated and shown). This is now improved, and all these aspects are now in consistency.**

Page 926, line 29 – Page 927, line 3 and also Page 928, lines 24-28. The statements attributed to Mueller et al (2012) in the current work seem much more specific than how I interpret what Mueller et al actually said. I believe that they see discrepancies between AERONET and in situ measurements which they partially attribute to the spheroidal model, but I do not see where they quantify an upper bound on the difference this can make, or a specific statement that this is due to the phase function at 180 degrees (although they do say less specifically, "the AERONET models were not designed to work at 180 degrees"). The statement in this manuscript implies that

20% is a theoretical upper bound, but Mueller et al. (2012) is an empirical study and doesn't make any theoretical explanation that would allow for a determination of an upper bound.

**If one looks at the SAMUM observations (Mueller et al., 2012, Gasteiger et al., 2011) and the measured depolarization ratio is always about 31% and the computed one is always not higher than 25% by using this spheroidal model, then the bias is 20%. If the lidar ratio is always 50-55sr, and the computed ones (based on the spheroidal model) are around 60-65sr, then the bias is again up to 20%. To further corroborate our impression, we show now the backscatter-related, extinction-related, and lidar-ratio-related Angstrom exponents, and the found discrepancies between the directly measured Angstrom values and the computed ones (based on the**

**spheroidal model) show the same features as shown by Mueller et al., 2012 and Gasteiger et al., 2011. All this now stated in the text.**

Page 926-927. The two paragraphs starting at the end of 926 and ending near the end of 927 list several possible explanations for a systematic bias between the LIRIC and POLIPHON results. You could learn more about the likelihood of some of these possibilities with relatively easy follow-up analysis. First, you note (here and elsewhere) the possibility of a discrepancy between the LIRIC coarse vs. fine partitions and the Raman spherical vs. non-spherical partitions. It seems to me that you have the means to compare like quantities. Given the four concentrations introduced in Eqns 5 and 6, it should be easy to compute the spherical and non-spherical fractions from LIRIC to make a more direct comparison with POLIPHON. Then you could know for sure if this explanation is applicable in these cases.

**We thank the reviewer for this idea to compare directly LIRIC (spherical, non-spherical particles) results with the POLIPHON (spherical, non-spherical particles) results. This leads to the improvement of Figures 4, 5, 10, and 11. Now the sphericity parameter (from AERONET) comes into play and is a very important quantity. This parameter is uncertain and thus the results. In the Saharan dust case the sphericity is 1.7% (LIRIC) and about 9% (POLIPHON). In the complex volcanic case, the LIRIC value is 15%, and the POLIPHON value is 55%. The POLIPHON results are more reasonable than the LIRIC/AERONET values as discussed in the result section.**

You also propose that the pure dust depolarization ratio might be too low. A sensitivity test could determine how big this value would have to be to produce good agreement. If the answer is about 34% or less, that would support this possible explanation, but if it would have to be much larger, it seems unlikely. Finally, you point out that the column value of backscatter and extinction used in the LIRIC analysis may not be an adequate representation of the height-dependent values. The Raman lidar provides fully resolved lidar measurements of height-dependent backscatter and extinction measurements. Is there any way to use these to check this possible explanation?

**We compare all the directly measured backscatter, extinction, lidar ratio, Angstrom, and depolarization ratio profiles, find partly agreement and partly not. This is extensively discussed, and discrepancies can be well explained. In the case of the simple Saharan dust case, all the discrepancies point to the use of the spheroidal model.**

Page 928, line 22-23. Discrepancy in the lidar ratio is referred back to the discussion that the 180 degree phase function in the spheroid model would lead to errors in the backscatter but not extinction. To address this, first of all, you should show a comparison of extinction. But I'm not sure I believe this explanation, because in this case the lidar ratio agreement is poor and the backscatter agreement is good (implying perhaps that the extinction agreement is poor).

**No, intensive quantities are clearly of advantage when comparing different results obtained with different methods. Now we compare even the wavelength dependence of the lidar ratio, and find that LIRIC/AERONET fails to determine the spectral slope of the dust lidar ratio. Again a clear sign that the spheroidal particle model is not adequate.**

Page 929, line 2. Lidar ratios of 78-80 sr at 355 nm seem very high. Mueller et al (2012) also saw a similar problematic result for the AERONET results in that study.

**And our final results show all this again and the lidar-ratio-related Angstrom exponents show this too, so all our results are in agreement with Mueller et al., 2012, and clearly indicate that the error source is most probably the spheroidal shape model.**

Page 929, line 10, “good agreement”. The agreement is not terrible, but the following discussion suggests that the depolarization should be almost a reproduction of the input profile, and it is not that good. Is there a reason for the high bias in the lower part of the dust layer and low bias in the upper part?

**We improved the discussion, and provide a more critical view.**

Page 933, lines 1-5: Note that the poor agreement in the previous graphs was below the lowest altitude Raman values in these graphs. There’s nothing to indicate that these results aren’t also poor at low altitudes, so the “surprisingly” good agreement is not necessarily a contradiction.

**The discussion is changed and consistent now based on the re-analyzed and additional Figures.**

Page 933, line 9: Please consider adding “using a combination of backscatter lidar and photometer measurements” or some similar phrase to the end of the sentence.

**Done!**

Page 933, line 14-15: This may be too strongly worded. In the discussion, the mass concentration comparison for the volcanic aerosol was described as acceptable considering the large error bars, which sounds less confident than “good and trustworthy”. The mass concentration comparison for the dust case was better. Being more specific about the differences between the cases (as suggested in the General Comments) would be good. Also since no comparison was made with the volume concentration, it is misplaced in this sentence.

**We changed the discussion accordingly. We also say at different places that clear conclusions on the LIRIC potential and uncertainty (including specification of error sources) is only possible in simple aerosol cases such as the Saharan dust case. This is not possible in the case of complex aerosol mixing and layering. Too many (or more or less all) assumptions made in LIRIC are then violated and at the end a clear uncertainty source identification is simple impossible. But again, we show more results now (especially the new Angstrom exponent figures). All the results underline how difficult a discussion on errors then is. To avoid speculation we have to leave such detailed discussions out. We say that, and conclude in the summary section: It is too early for final statements, we need more studies and comparisons....**

Figures: What are the horizontal and vertical resolution of the profiles shown in the figures?

**LIRIC vertical resolution is 15m. Horizontal resolution? If wind is blowing with 10m/s and we average two hours of the signals, we average air masses over 70 km.**

Figure 9: I don’t understand why the fine and coarse mode portions from the LIRIC results don’t add up to the total backscatter coefficient below about 0.5 km. Here the coarse mode is 0, the fine mode is approximately 1 per Mm-sr and the total is nearly 3 per Mm-sr.

**This was one of the erroneous profiles we re-checked and substituted now.**

Figure 11: The small angstrom exponent below 1 km seems inconsistent with the result that it is entirely fine mode with no coarse mode at that altitude. Is there an explanation for this?

**All this is now improved and consistent (optical versus microphysical properties).**

Technical Comments

Page 913, line 1-4: This is not a sentence. Was “analysis” meant to be “analyzes”? This would make it a sentence.

**Yes, we improved.**

Page 917, line 1: “RFOV”: Please spell out.

**Done!**

Page 918, line 8: missing word, “down to the”

**We improved.**

Page 925, line 7: suggest adding “the” to make “dominated the particle backscattering”. Page 929, line 6: suggest “is near zero” rather than “fluctuates around zero”.

**Done!**

# Evaluation of the Lidar/Radiometer Inversion Code (LIRIC) to determine microphysical properties of volcanic and desert dust

J. Wagner<sup>1</sup>, A. Ansmann<sup>1</sup>, U. Wandinger<sup>1</sup>, P. Seifert<sup>1</sup>, A. Schwarz<sup>1</sup>, M. Tesche<sup>2</sup>, A. Chaikovsky<sup>3</sup>, and O. Dubovik<sup>4</sup>

<sup>1</sup>Leibniz Institute for Tropospheric Research, Leipzig, Germany

<sup>2</sup>Department of Environmental Science, Stockholm University, Stockholm, Sweden

<sup>3</sup>Institute of Physics, National Academy of Science, Minsk, Belarus

<sup>4</sup>Laboratory of Atmospheric Optics, University Lille 1, Villeneuve d'Ascq, France

**Abstract.** The Lidar/Radiometer Inversion Code (LIRIC) combines the multiwavelength lidar technique with sun-sky photometry and allows us to retrieve vertical profiles of particle optical and microphysical properties, separately for fine-mode and coarse-mode particles. After a brief presentation of the theoretical background, we evaluate the potential of LIRIC to retrieve the optical and microphysical properties of irregularly shaped dust particles. The method is applied to two very different aerosol scenarios, a strong Saharan dust outbreak towards central Europe and an Eyjafjallajökull volcanic dust event. LIRIC profiles of particle mass concentrations for the coarse-mode as well as for the non-spherical particle fraction are compared with results for the non-spherical particle fraction as obtained with the polarization-lidar-based POLIPHON method. Similar comparisons for fine-mode and spherical particle fractions are presented, too. Acceptable agreement between the different dust mass concentration profiles is obtained. LIRIC profiles of optical properties such as particle backscatter coefficient, lidar ratio, Ångström exponent, and particle depolarization ratio are compared with direct Raman lidar observations. Systematic deviations between the LIRIC retrieval products and the Raman lidar measurements of the desert dust lidar ratio, depolarization ratio, and spectral dependencies of particle backscatter and lidar ratio point to the applied spheroidal particle model as main source for these uncertainty in the LIRIC results.

## 1 Introduction

The recent Icelandic volcanic eruptions in 2010 and 2011 emphasized the importance of remote-sensing methods that allow the separation of fine-mode and coarse-mode particles in the troposphere as a function of height (Ansmann et al.,

2011a, 2012). From the point of view of atmospheric research, there is a strong request for vertically resolved observations of optical and microphysical properties of atmospheric aerosols to improve our understanding of direct and indirect effects of aerosols on climate-relevant processes. The aerosol influence can be very different in the polluted boundary layer and in the free troposphere due to different aerosol lifetimes, transport ways and ranges, and interaction with low, midlevel, and high clouds.

Presently, efforts are undertaken in the framework of the European Aerosols, Clouds and Trace gases Research Infrastructure Network (ACTRIS) to make complementary use of different measurement techniques such as lidar (aerosol vertical profiling) and sun-sky photometry (spectrally resolved optical aerosol characterization) at combined European Aerosol Research Lidar Network (EARLINET) and Aerosol Robotic Network (AERONET) stations. The recently developed Lidar/Radiometer Inversion Code (LIRIC) was designed as a universal code for processing lidar/photometer network data, applicable to many different instrumental conditions and technical approaches. As outlined in Sect. 2, LIRIC uses profiles of elastic-backscatter lidar return signals at 355, 532, and 1064 nm and, as *a priori* assumptions, AERONET photometer retrieval products (column-integrated particle size distributions, composition, complex refractive index, and particle shape) (Chaikovsky et al., 2008, 2012). Products of this synergistic data analysis are height profiles of particle backscatter and extinction coefficients at the three wavelengths, and particle volume and mass concentration profiles separately for fine-mode and coarse-mode particles. Main goal of the LIRIC approach is to create a height-resolved data set of particle optical and microphysical properties which is in full agreement with the respective column-integrated findings from the sun-sky photometer observations. The method has been developed in a cooperation between the Institute of Physics Minsk (Belarus) and the Laboratoire d'Optique Atmosphérique Lille (France)

(Chaikovsky et al., 2008, 2012). The recently introduced Generalized Aerosol Retrieval from Radiometer and Lidar Combined Data (GARRLiC) (Lopatin et al., 2013) can be regarded as an extended version of LIRIC. The GARRLiC concept pursues an even deeper synergy of lidar and radiometer data in the retrievals, e.g., by using the lidar profile information to improve the AERONET retrievals.

There have been similar attempts to combine passive spaceborne remote sensing of aerosols with lidar aerosol profiling. Léon et al. (2003), Kaufman et al. (2003a), and Kaufman et al. (2003b) combined lidar observations of height profiles of particle backscattering with column-integrated spectral radiances measured with MODIS (MODerate resolution Imaging Spectroradiometer) to retrieve profiles of particle optical properties which are consistent with the microphysical properties from the MODIS observations. The third group of retrieval methods to derive microphysical particle properties are solely based on multiwavelength lidar observations of particle extinction and backscatter coefficients (Müller et al., 1999; Veselovskii et al., 2002; Böckmann et al., 2005). Recently these inversion techniques were extended to cover also desert dust observations and dust/smoke/sulfate aerosol mixtures (Veselovskii et al., 2010; Müller et al., 2013).

All these retrieval methods above are based on the assumption that the optical properties of the non-spherical, irregularly shaped coarse dust particles (desert dust, volcanic dust) can be sufficiently well described by assuming an ensemble of randomly oriented spheroidal dust particles with homogeneous mineralogical composition throughout the dust particle size distribution. However, prolate and oblate particles of different size are only approximations of the true shape of mineral dust particles. The exact shape of the dust particles cannot be described in this way. Ellipsoids have smooth surfaces, in contrast to the dust particles. Inclusions of various minerals in the dust grains and heterogeneous chemical composition are also not accounted for (Müller et al., 2013). Gasteiger et al. (2011a) pointed out that in addition to the shape effects, the assumption on the mineralogical composition (i.e., on the external and internal mixture of light-absorbing and non-absorbing dust particles) also have a very sensitive influence on the backscattering efficiency of dust particles.

The concept of describing the non-spherical component as an ensemble of randomly oriented spheroids with size-independent aspect-ratio (length-to-width-ratio) distribution has been successfully employed in the operational retrieval algorithm of AERONET (Dubovik et al., 2006). However, the central question remains: Is that model also appropriate for lidar applications which are based on backscattering by particles at exactly  $180^\circ$  scattering angle? The lidar inversion methods mentioned above were developed to retrieve microphysical properties of spherical aerosol particles (urban haze, fire smoke). Müller et al. (2013) state that the main reason for not using the spheroidal particle model for mineral

dust data is rooted in the poor understanding of how to describe the  $180^\circ$  light-scattering properties of particles of irregular (non-spherical) shape. The authors further state: We still look for theoretical models that allow us to link specific features of a particle's shape to its specific optical properties such as the measurable shape-sensitive particle extinction-to-backscatter ratio (lidar ratio) and the particle depolarization ratio. The lidar observations performed during the Saharan Mineral Dust Experiment (SAMUM) campaigns corroborate that the spheroidal particle model may not be adequate for lidar applications (Müller et al., 2010b; Ansmann et al., 2011b; Gasteiger et al., 2011a; Müller et al., 2012).

Here we investigate the potential of LIRIC to retrieve profiles of desert and volcanic dust optical properties such as the lidar ratio and depolarization ratio and microphysical properties such as particle volume and mass concentrations. Fortunately, independent remote-sensing methods are available that enable us to directly and simultaneously measure lidar ratio and depolarization ratio profiles by using the Raman/polarization lidar technique and to retrieve particle volume and mass concentrations of fine-mode and coarse-mode particles by means of the Polarization Lidar Photometer Network (POLIPHON) method (Ansmann et al., 2011a, 2012). These methods are also explained in Sect. 3. The POLIPHON technique is based on the measured height profile of the particle depolarization ratio to separate coarse dust from the residual aerosol particles and does not make use of the spheroidal particle model. However, the POLIPHON products contain uncertainties as well, especially for mixed aerosol cases, as will be discussed in Sect. 4.

We focus on two cases with aerosol layers containing a considerable amount of irregularly shaped coarse-mode particles. The first case refers to a strong Saharan dust outbreak towards Europe in May 2008. The second case covers the aerosol conditions after the eruption of the Icelandic volcano Eyjafjallajökull in April 2010. Section 2 describes the measurement systems. The LIRIC method is explained in Sect. 3. In addition, the basic idea of the POLIPHON method is briefly outlined. In Sect. 4, results are presented and discussed. Section 5 contains summarizing and concluding remarks.

## 2 Measurement systems

### 2.1 Raman lidar MARTHA

The multiwavelength Raman lidar MARTHA (Multiwavelength Atmospheric Raman lidar for Temperature, Humidity, and Aerosol profiling) is used for regular aerosol observations at the EARLINET station of Leipzig (Mattis et al., 2004). It provides height profiles of particle backscatter and extinction coefficients, lidar ratios as well as the volume and particle depolarization ratio (Ansmann et al., 1992, 2011a). Because Raman lidar signals are used (in addition to elastic-

backscatter signals), the method works best at darkness in the absence of strong sky background radiation. However, during events with optically dense aerosol layers, the Raman-lidar method for separate extinction and backscattering profiling can even be applied during daylight hours, as will be shown in Sect. 4.

For LIRIC, the elastically backscattered signals at the three transmitted wavelengths of 355, 532, and 1064 nm and the cross-polarized signal at 532 nm are used. LIRIC was originally designed for the analysis of lidar measurements at the three wavelengths of 355, 532, and 1064 nm. It has been extended to cover polarization lidar observations as well. MARTHA transmits linearly polarized laser light at 532 nm and has two channels to measure the cross-polarized lidar return signal  $P^\perp(\lambda, z)$  (the polarization-sensitive filter element is aligned orthogonal to the plane of laser beam polarization) and the total (cross and parallel-polarized) backscatter light  $P^\perp(\lambda, z) + P^\parallel(\lambda, z)$  with a second channel. From these signals the depolarization ratio (introduced in the next section) can be determined. Non-spherical particles such as desert or volcanic dust particles cause significant depolarization (a significant signal  $P^\perp$ ), whereas spherical particles and even fine-mode urban haze particles produce almost no cross-polarized backscatter.

The Raman signals are not used in the LIRIC scheme. However, the products of the Raman lidar measurements (backscatter, extinction, lidar ratio, depolarization ratio) are used in the LIRIC validation study. A direct comparison between the LIRIC and Raman lidar profiles provides the best opportunity to validate the LIRIC efforts.

For an optimum application of the LIRIC method, i.e., combining spectral tropospheric column with tropospheric profile information, it is necessary that the lidar covers almost the entire tropospheric column (as seen by the photometer) with profile observations. However, the incomplete overlap between the transmitted laser beams and the receiver field of view (RFOV) prohibits the measurement of reliable lidar return signals in the near range (usually up to a few 100 m, in the case of MARTHA up to a few kilometers because of the large telescope). The overlap function of our lidar is routinely and regularly determined and checked during clear nights with low aerosol amount by means of the method discussed by Wandinger and Ansmann (2002). The overlap profile is then applied to the aerosol lidar observations and allows us to correct the overlap effect usually down to heights of 500–1000 m above the lidar. Under favorable conditions (as for the Saharan dust case presented here), the overlap correction is reliable down to low minimum measurement heights of 150 m. Because the overlap effect may change from one to another lidar alignment which is routinely done in the beginning of each long-lasting lidar measurement session, different experimentally determined overlap profiles are used to check and quantify the impact of potential overlap uncertainties on the LIRIC retrieval accuracy.

## 2.2 Sun-sky photometer

LIRIC makes use of photometer-derived particle parameters that link the particle volume concentration to particle backscattering and extinction at 355, 532, and 1064 nm. The AERONET sun-sky photometers detect direct sun, aureole, and sky radiance (Holben et al., 1998). At Leipzig, direct sun radiation is measured in eight channels centered at wavelengths of 339, 379, 441, 501, 675, 869, 940, 1021, and 1638 nm. Sky radiation is obtained in four bands centered at 441, 675, 869, and 1021 nm. From direct sun measurements the aerosol (particle) optical thickness (AOT) and the Ångström exponent which describes the AOT wavelength dependence is derived. Sun and sky radiance observations are used for inversion algorithms to retrieve microphysical aerosol properties such as the volume particle size distribution for fine and coarse mode (Dubovik and King, 2000; Dubovik et al., 2006). The AERONET data analysis code searches for the minimum in the bimodal particle volume size distribution in the particle radius range from 0.194–0.576  $\mu\text{m}$ . The found minimum is used as a separation radius between fine-mode and coarse-mode particles. The complex refractive index and the contribution of spherical particles to the fine-mode and coarse-mode particle fractions are determined in addition. The wavelength-dependent refractive index is the same for both fine and coarse particles. In summary, from the retrieved information, AOTs, particle scattering phase functions, asymmetry parameters, and column volume and surface-area concentrations of the particles are derived for spherical and non-spherical particles of the fine-mode and the coarse-mode fractions (Dubovik et al., 2006). In cases without sky radiance observations, the AOTs and the column volume concentrations for fine and coarse mode are derived from the spectral dependence of measured AOT (O'Neill et al., 2003). The case studies in Sect. 4 are based on the Dubovik method.

The inversion of AERONET sky radiance measurements to obtain microphysical aerosol properties is well established (Dubovik and King, 2000; Dubovik et al., 2002, 2006). Besides these products, column values of the volume-specific backscatter and extinction coefficients separately for spherical and non-spherical particles in the fine-mode as well as in the coarse-mode can be estimated. These volume-specific backscatter and extinction values are important input data for LIRIC.

The spheroidal particle model as introduced by Dubovik et al. (2006) is successfully applied to the inversion of AERONET sun-sky photometer data to properly derive microphysical properties of desert dust. However, the way the spheroidal particle model influences the AERONET retrievals of dust properties is quite different from the way, the spheroidal particle model influences lidar applications and therefore the LIRIC results. In the case of AERONET, the complete phase function is fitted to the almucantar sky-brightness data such that the phase function reproduces the

almucantar data. In contrast, lidar backscatter data are repre-  
 285 sentative of the sky brightness at just one scattering angle of  
 exactly  $180^\circ$ . Whether the spheroidal particle model is appli-  
 cable to lidar observations remains an open question as dis-  
 cussed in the introduction. Uncertainties in the estimation of  
 volume-specific backscatter and extinction coefficients, re-  
 290 quired for LIRIC, arise also from the fact that sun-sky pho-  
 tometer measurements of almucantar usually end at a  $150^\circ$   
 scattering angle. The AERONET model was extended to a  
 phase function angle of  $173^\circ$  on the basis of laboratory mea-  
 surements of light scattering by dust (Volten et al., 2001).  
 295 Direct observations of the sky brightness at  $180^\circ$  scattering  
 angle cannot be made, so that all lidar-backscatter-related  
 AERONET values are model-based quantities.

### 3 Method

#### 3.1 Data preparation and processing

300 The basic structure of LIRIC is shown in Figure 1. In our  
 study we used the LIRIC version from autumn 2012. The  
 lidar database for LIRIC consists of background-corrected,  
 elastic-backscatter lidar signals  $P(\lambda_j, z_i)$  for different laser  
 wavelengths  $\lambda_j$ :

$$305 P(\lambda_j, z_i) = E_0(\lambda_j) \frac{O(\lambda_j, z_i)}{z_i^2} [\beta_{\text{aer}}(\lambda_j, z_i) + \beta_{\text{mol}}(\lambda_j, z_i)] \\ \times \exp \left\{ -2 \int_0^{z_i} [\alpha_{\text{aer}}(\lambda_j, z) + \alpha_{\text{mol}}(\lambda_j, z)] dz \right\}. \quad (1)$$

$E_0$  is the system constant and considers, e.g., the outgo-  
 ing laser pulse energy, collection area of the telescope, op-  
 310 tical efficiencies of the transmitter and receiver units, pho-  
 ton detection efficiency, and vertical thickness  $\Delta z$  of the  
 backscattering range cell.  $O(\lambda_j, z_i)$  describes the incom-  
 plete overlap of the laser beam for wavelength  $\lambda_j$  with the  
 RFOV.  $z_i$  denotes the vertical range between the lidar and  
 the backscattering range cell. The near-range measurements  
 are influenced by the changing laser-beam RFOV overlap.  
 This effect is corrected by use of measured overlap functions  
 $O(\lambda_j, z_i)$  as mentioned in Sect. 2.1.  $\beta_{\text{aer}}$  and  $\beta_{\text{mol}}$  are the  
 particle and Rayleigh backscatter coefficients and  $\alpha_{\text{aer}}$  and  
 315  $\alpha_{\text{mol}}$  the particle and Rayleigh extinction coefficients, re-  
 spectively. Besides the three elastic-backscatter signals the  
 cross-polarized lidar return at  $\lambda_2 = 532 \text{ nm}$

$$320 P^\perp(\lambda_2, z_i) = E_0(\lambda_2) \frac{O(\lambda_2, z_i)}{z_i^2} [\beta_{\text{aer}}^\perp(\lambda_2, z_i) + \beta_{\text{mol}}^\perp(\lambda_2, z_i)] \\ \times \exp \left\{ -2 \int_0^{z_i} [\alpha_{\text{aer}}(\lambda_j, z) + \alpha_{\text{mol}}(\lambda_j, z)] dz \right\} \quad (2)$$

is used.

After range and overlap correction the four signals are av-  
 325 eraged over a given time period (of minutes to hours, depend-  
 ing on the variability of the aerosol conditions) to increase  
 the signal-to-noise ratio. The corrected lidar signals

$$P_{\text{cor}}^p(\lambda_j, z_i) = \frac{P^p(\lambda_j, z_i) z_i^2}{O(\lambda_j, z_i)} \quad (3)$$

form the basic lidar input data set in the LIRIC data anal-  
 340 ysis. Here  $P^p(\lambda_j, z_i)$  with  $p = \parallel + \perp$  or  $p = \perp$  denotes the  
 total backscatter signal and the cross-polarized signal (for  
 $\lambda = 532 \text{ nm}$ ), respectively. For simplicity, we omit index  $p$  in  
 terms (as in Eq. (1) when  $p = \parallel + \perp$ ).

The minimum measurement height  $z_{N_0}$  and the refer-  
 ence height  $z_N$  must be defined. For heights below  $z_{N_0}$ ,  
 the retrieval assumes constant microphysical and height-  
 independent particle backscatter and extinction conditions as  
 large as the values observed at the minimum measurement  
 345 height (Mattis et al., 2004). Above  $z_N$  the contribution of  
 aerosol particles to the AOT is assumed to be negligible.

The following quantities are then introduced in the LIRIC  
 procedure (see Figure 1, green box):

$$L^{*p}(\lambda_j, z_n) = \frac{P_{\text{cor}}^p(\lambda_j, z_n)}{P_{\text{cor}}^p(\lambda_j, z_N)} [\beta_{\text{aer}}^p(\lambda_j, z_N) + \beta_{\text{mol}}^p(\lambda_j, z_N)] \\ \times \exp \left[ -2 \sum_{i=N}^{n+1} \alpha_{\text{mol}}(\lambda_j, z_i) \Delta z \right] \quad (4) \\ = [\beta_{\text{aer}}^p(\lambda_j, z_n) + \beta_{\text{mol}}^p(\lambda_j, z_n)] \\ \times \exp \left[ 2 \sum_{i=N}^{n+1} \alpha_{\text{aer}}(\lambda_j, z_i) \Delta z \right],$$

with the vertical range cell  $\Delta z$  which describes the range  
 resolution of the lidar measurement.  $L^*(\lambda_j, z_n)$  and  
 $L^{*\perp}(\lambda_2, z_n)$  can be easily computed from the measured sig-  
 355 nal ratios by using height profiles of Rayleigh backscatter  
 and extinction coefficients. The actual molecular optical  
 properties are obtained from atmospheric temperature and  
 pressure profiles by using a standard atmosphere model, in-  
 formation from a nearby radiosonde, or numerical weather  
 prediction products. In this study, we applied the U.S. stan-  
 dard atmosphere model and adjusted it to actual surface  
 temperature and pressure observations. The cross-polarized  
 Rayleigh backscatter coefficient  $\beta_{\text{mol}}^\perp$  contributes  $<1\%$   
 to the total molecular backscatter coefficient. Negligible par-  
 ticle depolarization ( $\beta_{\text{aer}}^\perp = 0$ ) is assumed at the reference  
 height  $z_N$ . As a LIRIC start value at  $z_N$ , we assume a  
 backscatter ratio of total (particle + Rayleigh) to Rayleigh  
 backscattering of 1.1 at  $z_N$  for all three wavelengths. How-  
 360 ever, the final backscatter and extinction profiles may not  
 show these backscatter ratios of 1.1 at height  $z_N$  at the end  
 of the LIRIC data analysis. The LIRIC code is designed  
 as a Least-Square-Method-based statistically optimized re-  
 trieval procedure (Dubovik and King, 2000; Dubovik, 2004)  
 370 as explained below and searches for lidar profiles of parti-  
 cle optical and microphysical properties that best match the

AERONET column-integrated findings. The calculation of  $L^*(\lambda_j, z_n)$  and  $L^{*\perp}(\lambda_2, z_n)$  starts from  $z_n = z_{N-1}$  downward towards the minimum measurement height  $z_{N_0}$  with a resolution of 15 m.

Eq. (4) shows that  $L^*(\lambda_j, z_n)$  and  $L^{*\perp}(\lambda_2, z_n)$  are mainly determined by height profiles of particle optical properties. These aerosol profiles are also estimated by means of aerosol products retrieved from the photometer observations. Comparing these profiles to the lidar measurements allows us to retrieve profiles of the particle volume concentrations. For this task, the expressions  $L(\lambda_j, z_n)$  and  $L^\perp(\lambda_2, z_n)$  similar to  $L^*(\lambda_j, z_n)$  and  $L^{*\perp}(\lambda_2, z_n)$  from Eq. (4) are introduced (see Figure 1, orange box):

$$L^P(\lambda_j, z_n) = [\beta_{\text{aer,e}}^P(\lambda_j, z_n) + \beta_{\text{mol}}^P(\lambda_j, z_n)] \times \exp \left[ 2 \sum_{i=N}^{n+1} \alpha_{\text{aer,e}}(\lambda_2, z_i) \Delta z \right]. \quad (5)$$

The particle backscatter and extinction coefficients  $\beta_{\text{aer,e}}$  and  $\alpha_{\text{aer,e}}$  (index e for estimate from photometer observations), respectively, are defined as

$$\beta_{\text{aer,e}}(\lambda, z) = C_{f,1}(z)b_{f,1}(\lambda) + C_{f,2}(z)b_{f,2}(\lambda) + C_{c,1}(z)b_{c,1}(\lambda) + C_{c,2}(z)b_{c,2}(\lambda), \quad (6)$$

$$\beta_{\text{aer,e}}^\perp(\lambda, z) = C_{f,2}(z)b_{f,2}^\perp(\lambda) + C_{c,2}(z)b_{c,2}^\perp(\lambda), \quad (7)$$

$$\alpha_{\text{aer,e}}(\lambda, z) = C_{f,1}(z)a_{f,1}(\lambda) + C_{f,2}(z)a_{f,2}(\lambda) + C_{c,1}(z)a_{c,1}(\lambda) + C_{c,2}(z)a_{c,2}(\lambda) \quad (8)$$

with the particle volume concentrations  $C_{m,s}(z)$  for particle mode  $m$  (index f for fine mode and index c for coarse mode) and particle shape parameter  $s$  with  $s = 1$  for spherical particles and  $s = 2$  for non-spherical particles.  $C_{m,s}(z)$  are the variables that have to be optimized in the LIRIC data analysis. The procedure is outlined in detail in Chaikovsky et al. (2008, 2012) and Wagner (2012). In Eqs. (6)–(8), the column mean values of the volume-specific particle backscatter coefficients  $b$  and  $b^\perp$  and extinction coefficient  $a$  are defined as (see Figure 1, yellow boxes to the left)

$$b_{m,s}^P(\lambda) = \frac{\tau_{\text{ext},m,s}(\lambda)\omega_{m,s}(\lambda)F_{m,s}^P(\lambda, \Theta = 180^\circ)}{4\pi V_{m,s}}, \quad (9)$$

with

$$F_{m,s}(\lambda, \Theta = 180^\circ) = F_{11,m,s}(\lambda, \Theta = 180^\circ), \quad (10)$$

$$F_{m,2}^\perp(\lambda_2, \Theta = 180^\circ) = \frac{1}{2} [F_{11,m,2}(\lambda_2, \Theta = 180^\circ) - F_{22,m,2}(\lambda_2, \Theta = 180^\circ)], \quad (11)$$

and

$$a_{m,s}(\lambda) = \frac{\tau_{\text{ext},m,s}(\lambda)}{V_{m,s}}. \quad (12)$$

$F_{11}$  and  $F_{22}$  are the first and second diagonal elements of the scattering matrix, respectively,  $\tau_{\text{ext}}$  denotes the extinction optical thickness, and  $\omega$  the single-scattering albedo. From

photometric measurements (see Figure 1, yellow box) the retrieved fine-mode and coarse-mode volume concentrations  $V_{m,s}$ , the complex refractive index (real part  $n_r$ , imaginary part  $n_i$ ), the size distribution, and the volume fractions of spherical particles (denoted as sphericity in the AERONET data base) are required to solve Eqs. (9)–(12). These quantities are obtained by means of the AERONET inversion algorithm. The non-spherical particles are described with the spheroidal particle model after Dubovik et al. (2006).

Several simplifying assumptions are made. The refractive-index characteristics is the same for fine and coarse particles. The ratio of spherical to spheroidal particles (in terms of volume concentration) is also assumed to be the same for fine mode and coarse mode. However, the ratio can vary with height in the case of coarse-mode particles in accordance with the vertical distribution of non-spherical particles as indicated by the cross-polarized 532 nm backscatter signal. The ratio of spherical to spheroidal particles is height-independent for fine-mode particles in order to keep the set of input parameters as small as possible. Under the assumption of randomly oriented spheroids in the particle mixture  $F_{11}$ ,  $F_{22}$ ,  $\tau_{\text{ext}}$ , and  $\omega$  are provided for the lidar wavelengths by solving the vector radiative-transfer equation for a plane-parallel multi-layered atmosphere (Dubovik et al., 2006).

These simplifications may introduce considerable uncertainties, e.g., when spherical sulfate particles (fine mode) are present in the vertical column together with irregularly shaped volcanic dust particles (coarse mode) so that the refractive-index characteristics as well as the ratio of spherical to non-spherical particles are very different for fine and coarse particle fractions. Such a situation occurred after the Eyjafjallajökull volcanic eruption and is discussed in the next section.

It remains to be mentioned that  $b_{m,s}(\lambda)$  can be expressed by  $a_{m,s}(\lambda)/S_{m,s}(\lambda)$  with the extinction-to-backscatter ratio (lidar ratio)

$$S_{m,s}(\lambda) = \frac{4\pi}{\omega_{m,s}(\lambda)F_{m,s}(\lambda, \Theta = 180^\circ)}. \quad (13)$$

The lidar ratio is an essential lidar parameter in the characterization of aerosol particle mixtures and types (Müller et al., 2007).

As mentioned, LIRIC is based on the Least Square Method (LSM) for the statistically optimized inversion of multi-source data (Dubovik and King, 2000; Dubovik, 2004). It is out of the scope of this paper to describe the entire LIRIC data processing scheme in detail. As part of the LIRIC optimization process the difference between the AERONET-related expression  $L^P(\lambda_j, z_n)$  and the lidar-derived expression  $L^{*P}(\lambda_j, z_n)$  is minimized with respect to the particle volume concentrations  $C_{m,s}$  (Figure 1, orange box, center). Also, the photometer-derived column volume concentrations  $V_{m,s}$  must agree with the corresponding integrals over the

respective concentration profiles (Figure 1, orange box, center):

$$V_{m,s} = C_{m,s}(z_{N_0})z_{N_0} + \sum_{i=N_0}^N [C_{m,s}(z_i)]\Delta z. \quad (14)$$

Here,  $C_{m,s}(z_{N_0})z_{N_0}$  describes the contribution of the lowermost tropospheric layer (below the lowermost lidar measurement height  $z_{N_0}$ ) to the volume concentration profile. For heights  $< z_{N_0}$  the values are set constant and equal to the value at  $z_{N_0}$ .

The LSM-based statistical retrieval procedure requires covariance matrices of the lidar signal measurement errors (as a function of height). Details to the signal noise estimations for the observations cases shown here are given by Wagner (2012). To assure optimized profiles, the optimization process is performed within the error margins following principles of statistical estimation theory (Eadie et al., 1971). More information about the LIRIC data analysis can be found in Chaikovsky et al. (2008, 2012) and Wagner (2012).

To characterize the uncertainties in the LIRIC results the input parameters are varied. In Sect. 4, only errors are shown (as error bars) that originate from the LIRIC data procedure itself and the related input (regularization parameters). To obtain a characteristic error introduced by the LIRIC method, 5–10 runs were performed with realistic, but well selected regularization parameter sets. These results were used in the estimation of the standard deviation of the entire uncertainty range (of possible LIRIC solutions).

Retrieval uncertainties caused by uncertainties in the input lidar profiles via uncertainties in the overlap correction, by selecting the minimum and maximum height of the LIRIC vertical range, and uncertainties in the particle backscatter coefficient at the reference height are discussed in Sect. 4 as well. However, the reference height is chosen in a range where particle backscattering does not contribute much to the lidar signal so that the impact on the uncertainty of the LIRIC results is low. The minimum height is selected such that the overlap correction above this height is trustworthy so that the influence of overlap correction uncertainties is kept as low as possible. The minimum measurement height is typically set into the lower to central part of the well-mixed boundary layer. The aerosol concentrations below the minimum height are assumed to be height-independent in the well-mixed layer, and the impact of this assumption on the retrieval uncertainty should therefore be small. In other words, these parameters are already optimized during the lidar signal preparation phase and values other than the chosen lidar data parameters would lead to worse and usually unreasonable results in terms of backscatter and extinction profile structures, and can thus easily be sorted out.

Finally, the mass concentrations  $M_f(z)$  and  $M_c(z)$  for fine-mode and coarse-mode particles, respectively, can be calculated from the particle volume concentrations  $C_{m,s}(z)$ :

$$M_f(z) = \rho_1 C_{f,1}(z) + \rho_2 C_{f,2}(z), \quad (15)$$

$$M_c(z) = \rho_1 C_{c,1}(z) + \rho_2 C_{c,2}(z). \quad (16)$$

Estimates of the particle densities  $\rho_1$  and  $\rho_2$  (assumed to be height-independent) are required. Appropriate values of  $\rho_1$  (mainly sulfate aerosol) and  $\rho_2$  (desert and volcanic dust) can be found, e.g., in Ansmann et al. (2012). The final products of the LIRIC data analysis are summarized in the blue box in Figure 1. To better compare the LIRIC results with the products of the POLIPHON method (Sect. 3.2), mass concentrations for spherical and non-spherical particles are computed in addition:

$$M_1(z) = \rho_1 [C_{f,1}(z) + C_{c,1}(z)], \quad (17)$$

$$M_2(z) = \rho_2 [C_{f,2}(z) + C_{c,2}(z)]. \quad (18)$$

From the LIRIC backscatter and extinction coefficients after Eqs. (6) and (8), the lidar ratio profiles for the different wavelengths can be computed,

$$S_{\text{aer,e}}(\lambda, z) = \frac{\alpha_{\text{aer,e}}(\lambda, z)}{\beta_{\text{aer,e}}(\lambda, z)}. \quad (19)$$

Several Ångström exponents (Ångström, 1961),

$$\mathring{\alpha}_{x_e}(\lambda_1, \lambda_2, z) = -\frac{\ln[x_e(\lambda_1, z)/x_e(\lambda_2, z)]}{\ln(\lambda_1/\lambda_2)}, \quad (20)$$

with  $\lambda_1 < \lambda_2$  can be calculated from the profiles of the particle backscatter ( $x_e = \beta_{\text{aer,e}}$ ) and extinction coefficients ( $x_e = \alpha_{\text{aer,e}}$ ).

The photometer data in combination with the applied particle scattering model (for spherical and spheroidal particles) permit the retrieval of column-mean backscatter coefficients as a function of the polarization state with respect to the incident laser light:

$$b^\perp(\lambda) = b_{f,1}^\perp(\lambda) + b_{f,2}^\perp(\lambda) + b_{c,1}^\perp(\lambda) + b_{c,2}^\perp(\lambda), \quad (21)$$

$$b^\parallel(\lambda) = b_{f,1}^\parallel(\lambda) + b_{f,2}^\parallel(\lambda) + b_{c,1}^\parallel(\lambda) + b_{c,2}^\parallel(\lambda). \quad (22)$$

For spherical particles the contributions to light depolarization are negligible so that  $b_{f,1}^\perp(\lambda) = 0$  and  $b_{c,1}^\perp(\lambda) = 0$ . As mentioned, only non-spherical particles (desert dust, volcanic dust) cause significant depolarization. Instead of Eq. (6), we can write:

$$\beta_{\text{aer,e}}^\perp(\lambda, z) = C_{f,2}(z)b_{f,2}^\perp(\lambda) + C_{c,2}(z)b_{c,2}^\perp(\lambda), \quad (23)$$

$$\beta_{\text{aer,e}}^\parallel(\lambda, z) = C_{f,1}(z)b_{f,1}^\parallel(\lambda) + C_{f,2}(z)b_{f,2}^\parallel(\lambda) + C_{c,1}(z)b_{c,1}^\parallel(\lambda) + C_{c,2}(z)b_{c,2}^\parallel(\lambda), \quad (24)$$

so that we finally obtain the particle linear depolarization ratio:

$$\delta_{\text{aer,e}}(\lambda) = \beta_{\text{aer,e}}^\perp(\lambda) / \beta_{\text{aer,e}}^\parallel(\lambda). \quad (25)$$

The photometer-derived profiles of the lidar ratio, Ångström exponents for backscatter and extinction, and depolarization ratio can be compared with the respective results directly determined from the Raman lidar observations (Ansmann et al.,

1992; Mattis et al., 2004; Tesche et al., 2009a). This comparison is presented in Sect. 4.

With respect to the retrieval of mass concentration for dust particles, we can summarize that LIRIC uses photometer-derived volume-specific backscatter and extinction coefficients for spherical as well as non-spherical particles for both fine and coarse modes. This AERONET information (column-integrated values) is then applied to determine height profiles of volume and mass concentration of spherical and non-spherical fine-mode particles and spherical and non-spherical coarse-mode particles by minimizing the differences between the modelled lidar profiles  $L(\lambda, z)$  and the measured lidar profiles  $L^*(\lambda, z)$ . The important point is that LIRIC is based on the assumption that non-spherical particles can be described by a spheroidal particle model. This may significantly affect the backscatter-coefficient, lidar-ratio, and depolarization-ratio retrievals (Gasteiger et al., 2011a; Müller et al., 2012), and thus the derived particle volume and mass concentrations. The implication of the model assumption on a spheroidal particle shape is discussed in Sect. 4 by comparing the LIRIC output with results obtained by means of the POLIPHON technique.

### 3.2 Determination of particle mass concentrations by means of the POLIPHON technique

An alternative approach for the retrieval of particle volume and mass concentration profiles is the single-wavelength POLIPHON technique (Ansmann et al., 2012). The method is based on measured profiles of the particle linear depolarization ratio and the lidar ratio at 532 nm and does not require the assumption of a specific particle shape. In this depolarization-ratio-based method it is assumed that the fine-mode-related backscatter and extinction coefficients are exclusively caused by non-depolarizing spherical particles (i.e., fine-mode fraction) and that the coarse mode consists of strongly light-depolarizing non-spherical particles only. Spherical coarse particles as well as non-spherical fine-mode particles are thus ignored in this method. If the particle depolarization ratio is  $\geq 0.31$  in Saharan dust layers, the fine-mode particle fraction is set to 0%. If the 532-nm depolarization ratio is  $\leq 0.02$ , the coarse-mode fraction is set to 0%. For depolarization ratios from 0.02 to 0.31 we use the method described by Sugimoto et al. (2003) and Tesche et al. (2009a) to compute the height profiles of the backscatter coefficient  $\beta_{\text{aer},1}$  of spherical particles and of  $\beta_{\text{aer},2}$  of non-spherical particles at  $\lambda = 532$  nm. For volcanic dust, the data analysis is the same, except the volcanic depolarization ratio is set to 0.34 (Ansmann et al., 2012).

As it is the case for the LIRIC method, the POLIPHON technique makes use of photometer-derived volume-specific extinction coefficients  $a_f$  and  $a_c$  for fine-mode and coarse-mode particles (Eq. (12)). The values for  $a_f$  and  $a_c$  can directly be computed from volume concentrations  $V_f$  and  $V_c$  and AOTs  $\tau_{\text{ext},f}$  and  $\tau_{\text{ext},c}$  downloaded from the AERONET

website. The parameters  $a_f$  and  $a_c$  are almost insensitive to particle shape effects (Dubovik et al., 2006), in contrast to scattering properties computed for a scattering angle of  $180^\circ$  (as required in the LIRIC data analysis). The reason is that small-angle forward scattering mainly contributes to particle extinction and that the corresponding phase function segments for spheroidal and spherical particles are very similar (Dubovik et al., 2006).

The mass concentrations  $M_1$  for spherical particles (fine mode) and  $M_2$  for non-spherical particles (coarse mode) are estimated as follows:

$$\begin{aligned} M_1(z) &= \rho_1 (\overline{V_f / \tau_{\text{ext},f}}) \beta_{\text{aer},1}(z) S_{\text{aer},1} \\ &= \rho_1 (\overline{a_f^{-1}}) \beta_{\text{aer},1}(z) S_{\text{aer},1}, \end{aligned} \quad (26)$$

$$\begin{aligned} M_2(z) &= \rho_2 (\overline{V_c / \tau_{\text{ext},c}}) \beta_{\text{aer},2}(z) S_{\text{aer},2} \\ &= \rho_2 (\overline{a_c^{-1}}) \beta_{\text{aer},2}(z) S_{\text{aer},2}. \end{aligned} \quad (27)$$

According to these equations, appropriate (actual) lidar ratios  $S_{\text{aer},1}$  and  $S_{\text{aer},2}$  are needed and obtained from the Raman lidar measurements or from combined photometer-lidar observations (Ansmann et al., 2011b, 2012). We use column lidar ratios in the mass concentration retrieval, disregarding that the Raman-lidar method provides lidar ratio profiles. Besides particle densities  $\rho_1$  and  $\rho_2$ , temporal mean values of the volume-to-extinction conversion factors  $\overline{V_{c,f} / \tau_{\text{ext},c,f}}$  are determined and inserted in Eqs. (26) and (27).

The main advantage of the POLIPHON method is that a particle shape model for irregularly shaped dust particles is not required. The particle depolarization ratio is used to separate spherical and non-spherical particle fractions. However, fine and coarse mode fractions as determined with LIRIC may not be well represented by these spherical and non-spherical particle fractions. A significant part of the non-spherical dust particles may belong to the fine mode, but are interpreted as coarse-mode particles when applying POLIPHON, i.e. when the non-spherical particle fraction is assumed to be identical with the coarse mode fraction. This aspect is further discussed in the next section.

Table 1 provides finally an overview of the essential atmospheric and lidar system parameters required in the LIRIC and POLIPHON volume and particle mass concentration retrievals. From this comparison the contrast between the methods becomes very clear. Overlap corrections are critical in LIRIC analysis because the lidar profiles as a whole are set into context with the column-integrated particle information from AERONET observations. Overlap effects affect the POLIPHON results only in the near range (incomplete overlap). Further important LIRIC assumptions are the spheroidal particle model and also the refractive-index characteristics because they sensitively influence the computation of the volume-specific backscatter coefficients (Gasteiger et al., 2011a) required in the LIRIC analysis scheme. As mentioned the volume-specific extinction coefficients used in both the LIRIC and the POLIPHON methods are almost

insensitive regarding particle shape effects (spheroidal versus spherical particle model) so that the POLIPHON results are favorable to study the influence of the applied spheroidal particle model on the LIRIC mass retrieval. The other assumptions and input parameters in Table 1 are less critical and introduce only minor uncertainties in the mass concentration retrieval. A critical aspect remains in the case of hygroscopic volcanic dust (Ansmann et al., 2012). As will be discussed below, at high relative humidities a part of the volcanic coarse dust may become spherical and may then be counted as fine-mode aerosol. Under these conditions, the volcanic dust concentrations will be underestimated.

## 4 Results

Two case studies are presented in the following. A strong Saharan dust outbreak reached central Europe in the end of May 2008. Anthropogenic and dust particles were almost perfectly separated with height. Urban haze occurred in the lowermost 700 m of the atmosphere, whereas desert dust was observed from 1–6 km height. Mixing was prohibited by a strong temperature inversion layer at the top of the haze layer. The fine-mode fraction (FMF, ratio of fine-mode AOT to total AOT) was 0.20–0.25 and the spherical-particle volume fraction (sphericity) was estimated by the AERONET retrieval to be 1.7%. Thus, practically all particles were irregularly shaped dust particles. Under these conditions, all simplifying LIRIC assumptions such as same refractive-index characteristics and same ratios of spherical to non-spherical particles in both particle modes are widely fulfilled so that optimum conditions are given to study the impact of the spheroidal particle model on the retrieved profiles of dust optical and microphysical properties.

In contrast, the second case observed over Leipzig after the Eyjafjallajökull volcanic eruption in April 2010 deals with an aged volcanically disturbed air mass with vertically complex aerosol layering and mixing of spherical sulfate particles (fine mode) and non-spherical volcanic dust particles (fine-mode and coarse-mode particles). The volcanic particles may have been partly spherical because of water uptake at high relative humidity. In contrast to the Saharan dust case, the FMF was close to 0.8. Fine-mode particles dominated particle backscattering and extinction. The contribution of spherical particles to the particle volume concentration was of the order of 15% according to the AERONET retrievals. Very different refractive-index characteristics and very different ratios of spherical-to-non-spherical particles in fine mode and coarse mode can be expected. All basic assumptions of the LIRIC/AERONET approach, as listed in Table 1, were probably considerably violated. This second, complex aerosol case may especially show the limits of the synergy of column-integrated and profile observations. These two observational cases were already discussed in detail by Ansmann et al. (2012) so that the LIRIC method can be applied

to well-documented and quality-checked lidar/photometer data sets.

### 4.1 Saharan dust

A long-lasting Saharan dust event was monitored with lidar and photometer from 25–31 May 2008. The particle optical thickness at 500 nm showed values around 0.7 from the early morning of 28 May 2008 to the early morning of 30 May 2008. Figure 2 shows lidar height–time displays of the 1064-nm range-corrected signal in the evening of 29 May 2008. Well stratified dust layers up to 5.5 km were found. Persistent, long-lasting cirrus decks frequently occurred and disturbed the AERONET sun–sky photometer observations. A good opportunity to compare and combine lidar and photometer observations and to apply the LIRIC method was given in the evening of 29 May 2008. At around 1730 UTC, the sky was cloud-free during several successive AERONET observations. Stable aerosol conditions (see discussion below) throughout the following night enabled the determination of the full set of Raman lidar results and ensured a perfect framework for a critical assessment of the LIRIC results.

Because of these very constant aerosol conditions we averaged all cloud-screened lidar profiles measured in the evening of 29 May 2008, 2147 to 2315 UTC, to minimize the impact of signal noise on the retrieval. The respective 1.5-hour mean profiles of the three particle backscatter coefficients at 355, 532, and 1064 nm computed with Eq. (6) and the corresponding extinction profiles after Eq. (8) are presented in Figure 3. In addition, the particle backscatter coefficient computed from the cross-polarized 532-nm backscatter signal is presented. This latter backscatter coefficient considers only backscattering by non-spherical particles according to Eq. (7). Figure 3 also shows the corresponding profiles of the volume concentrations for fine-mode and coarse-mode particles as retrieved with LIRIC. As mentioned, the vertically integrated fine-mode and coarse-mode volume concentrations must match the respective column values retrieved from AERONET observations.

As outlined above, the lidar was well aligned on this day and the overlap function well characterized. The incomplete overlap between laser beam and RFOV could be corrected with sufficient accuracy down to  $z_{N_0} = 150$  m height. The reference height  $z_N$  was set to 9 km height. The 500-nm AOT measured with the AERONET photometer was 0.73 at 1730 UTC and 0.70 in the next morning.

The particle backscatter coefficients show a weak reversed spectral order (negative Ångström exponent) in the dust layer between 500 m and 5.5 km height and almost no wavelength dependence in terms of the extinction coefficient. In the pollution layer below 600 m height, a strong decrease of the backscatter and extinction coefficients with wavelength is found according to Ångström values of around 1.5. The volume concentration profiles show a dominant coarse particle mode in the height range from 600 m to 6 km. The fine-

mode particles predominantly occur in the boundary layer below 600 m and another weak accumulation of fine particles is found around 2 km. The reversed backscatter spectrum in the dust layer may be caused by the use of the spheroidal particle model in the LIRIC/AERONET retrieval as further discussed below.

As mentioned the error bars in Figure 3 only account for uncertainties in the input parameters of the LIRIC procedure, and not for uncertainties in the basic lidar signal profiles. We estimated a potential impact of the overlap correction by using three different, but reasonable overlap profiles and found that the results shown in Figure 3 varied by up to 25% in the lowermost 1500 m and on the order of 5% in the aerosol layers up to 3500 m. Variations of the reference height and minimum measurement height in the LIRIC data analysis by  $\pm 1$  km lead to variations in the backscatter and extinction coefficients by up to 50% in the lowermost 1500 m and around 15% in the aerosol layers. However, many of these resulting LIRIC profiles then show, e.g., a constant, but unrealistic offset above the main aerosol layers (around the reference height) and can thus be sorted out by visual inspection. Nevertheless, a careful study of the impact of the overlap correction and setting of the minimum and reference heights is an important part of the lidar data analysis and an important prerequisite for high-quality LIRIC products.

Figure 4 shows a comparison of the LIRIC backscatter coefficients at 532 nm with respective backscatter profiles directly retrieved from the Raman lidar observations (total backscatter coefficient, for simplicity denoted as POLIPHON curves) and derived by using the separation method of Tesche et al. (2009a) for the spherical and non-spherical particle fractions. As can be seen, the total backscatter coefficients agree well. The respective 532 nm extinction coefficient in Figure 3 is however overestimated by 10%–20% in the dust layer when compared to the direct Raman lidar observation (not shown) and thus also the dust extinction-to-backscatter ratio is overestimated (more details are given below).

In the central and left parts of Figure 4, the LIRIC backscatter coefficient for non-spherical and spherical particles are shown and compared with the respective POLIPHON result. In addition, the LIRIC backscatter profiles for the fine mode and coarse mode are given. The sphericity as provided by the AERONET retrieval plays an important role in the LIRIC data analysis. The spherical particle volume fraction is 1.7% after AERONET and finally 0.1% in the LIRIC data set. According to the POLIPHON volume concentrations the sphericity is 8.5%. As a consequence, the LIRIC non-spherical particle backscatter coefficients are slightly larger than the respective POLIPHON values in the lofted Saharan dust layer and considerably larger in the haze layer below 700 m height. By comparing the LIRIC coarse-mode backscatter profile with the one for non-spherical particles we obtain an impression how much of the backscatter is caused by non-spherical fine-mode particles.

Because of the low AERONET sphericity value the backscatter coefficient for spherical particles is almost zero at all heights. In contrast, the respective POLIPHON curve shows that spherical particles considerably contributed to backscattering in the haze layer. This fine-mode backscatter in the lowermost 700 m is attributed to non-spherical particles after LIRIC (see center plot in Figure 4).

Figure 5 shows the LIRIC mass concentration profiles, separately for non-spherical and for spherical particles (Eqs. (17)–(18)) and for fine-mode and coarse mode (Eqs. (15)–(16)). The LIRIC profiles are compared with respective POLIPHON profiles for non-spherical and spherical particles (Eqs. (26)–(27)). Particle densities of  $\rho_2 = 2.6 \text{ g/cm}^3$  and  $\rho_1 = 1.6 \text{ g/cm}^3$  are assumed for non-spherical and spherical particles, respectively. As can be seen, a good agreement of the LIRIC and POLIPHON results for non-spherical and coarse-mode particles is found. The slightly larger LIRIC values are again caused by the low LIRIC sphericity value of 0.1% which leads to an overestimation of the non-spherical particle volume fraction (compared to the POLIPHON volume concentrations). This good agreement suggests that the non-spherical (light depolarizing) particle fraction well represents the coarse mode in the particle volume and mass retrievals in this case of a strong Saharan dust outbreak.

As a further consequence of the low AERONET sphericity value the mass concentration for spherical particles is almost zero (not visible in the right plot of Figure 5), whereas the POLIPHON approach suggests a considerable mass concentration of spherical, roughly as large as the LIRIC fine-mode mass concentration. The POLIPHON results are more realistic. It is at least unrealistic to assume that the mass concentration of non-depolarizing urban haze over the central European city of Leipzig was negligible in the lowermost 700 m of the atmosphere on this specific day with a huge Saharan dust outbreak.

The sphericity parameter is of central importance in the separation of dust (non-spherical particles) and non-dust volume and mass concentrations with the LIRIC method. The spheroidal particle model can thus be regarded as one uncertainty source leading to too low sphericity values. However, it is also possible that the POLIPHON pure dust depolarization ratio of 31% used in the separation of dust and non-dust aerosol components is too high. Lower threshold values (below 30%) lead to a decrease of the POLIPHON-derived sphericity, i.e., to an increase of the contribution of non-spherical particles to the observed optical effects. On the other hand, as will be discussed below, the use of the spheroidal particle model causes too low dust depolarization ratios when compared with directly measured depolarization ratios for desert dust (Müller et al., 2010b, 2012; Gasteiger et al., 2011a) and thus a too large sphericity value.

The applicability of the spheroidal particle model is further illuminated in Figures 6 and 7. LIRIC results for the intensive particle parameters such as particle lidar ratio, de-

polarization ratio, and Ångström exponents are shown and compared with direct Raman lidar observations. The 532 nm lidar ratios (LIRIC, Eq. (19)) are determined by dividing the 532 nm extinction coefficients by the 532 nm backscatter values in Figure 3. The Ångström exponents are computed from the 355, 532, and 1064 nm backscatter and 355 and 532 nm extinction coefficients in Figure 3 by means of Eq. (20). In the case of the LIRIC particle depolarization ratios, the backscatter coefficients computed from the cross-polarized and total signals shown in Figure 3 are used according to Eq. (25).

As can be seen, the particle lidar ratio in the dust layer and the spectral slope (or Ångström exponent) of the dust lidar ratio are systematically overestimated by the LIRIC/AERONET approach and correspondingly the backscatter-related Ångström exponent is clearly underestimated. In addition, the values of the particle depolarization ratio in the lofted dust layer are systematically lower than the directly measured ones. These discrepancies are in full agreement with the findings from the SAMUM observations in southern Morocco (Gasteiger et al., 2011a; Müller et al., 2010b, 2012). These deviations of LIRIC profiles from the measured values (Raman lidar) clearly point to the spheroidal particle model as main error source. Directly observed lidar ratios for 355 and 532 nm are around 50–55 sr in Figure 6. These values are typical for the western Saharan dust (Teschke et al., 2009b; Schuster et al., 2012). The LIRIC backscatter and extinction profiles lead to dust lidar ratios of 78–80 sr (355 nm) and 60–62 sr (532 nm) in the height range from 1500–3000 m (center part of the dust layer).

However, the lidar ratio (or better the particle backscatter coefficient) depends in a complicated way on the chemical composition (refractive-index characteristics), size distribution, particle shape, and aspect ratio (particle length-to-width ratio) distributions. It remains an open question to what extent the spheroidal particle model is responsible for the observed systematic bias in the Ångström exponents and lidar ratios. Furthermore, the *a priori* AERONET input data are provided as column values, ignoring the observed aerosol layering with a lofted dust aerosol layer above the central European haze layer. As a last point, in LIRIC the same refractive index is used for both fine-mode and coarse-mode particles, disregarding the fact that fine-mode sulfate particles and coarse-mode desert dust particles show different scattering and absorption properties including respective wavelength dependence.

The depolarization ratio strongly depends on particle shape. During SAMUM, dust depolarization ratios were around 0.23–0.25 (355 nm) and 0.30–0.35 (532 nm). Müller et al. (2010b, 2012) found 20% (355 nm) to 30% (532 nm) lower particle depolarization ratios from the SAMUM AERONET computations assuming spheroidal particles with smooth surfaces. Very similar deviations are shown in Figure 7. Gasteiger et al. (2011a) studied the depolarization ratios for spheroids with smooth surfaces and spheroids with

deformations (rough surfaces) based on modelling. The depolarization ratio increases by 20%–30% when spheroids with rough surfaces are assumed. Spheroids with surface deformations also better reproduce the measured lidar ratios (reducing the overestimation) than spheroidal particles with smooth surfaces. It remains to be mentioned that fine-mode spheroidal particles produce a particle depolarization ratio about 5%–6% as can be seen in Figure 6 (right panel) at heights below 500 m (LIRIC profiles).

## 4.2 Volcanic ash on 19 April 2010

In April 2010, an aged volcanic aerosol layer consisting of a mixture of volcanic dust, volcanic sulfate particles, and anthropogenic haze occurred over central Europe. These aerosol conditions provided a unique opportunity to apply the LIRIC approach to another type of irregularly shaped aerosol particles. In contrast to desert dust, volcanic dust is hygroscopic (Latham et al., 2011) so that changes in the shape characteristics by water uptake cannot be excluded when relative humidity is high (i.e., >70%) (Ansmann et al., 2012). As a consequence, spherical particles may occur not only in the fine-mode, but also in the coarse-mode fraction, and thus may complicate the interpretation of POLIPHON results and the comparison with LIRIC results. The contribution of spherical particles to the particle volume concentration was about 15% according to the AERONET data analysis.

The volcanic layers observed on 19 April 2010 originated from the Eyjafjallajökull volcanic eruptions on Iceland on 14 April 2010 (Ansmann et al., 2011a; Schumann et al., 2011). Figure 8 shows the situation in the afternoon of 19 April 2010. The 500 nm AOT was about 0.7, and the FMF about 0.8. The well-mixed boundary layer reached to 1000–1400 m height on that day. Above the boundary layer another layer of 1500 m thickness occurred mainly consisting of volcanic dust. Between 3.8 and 5.5 km height a further dust layer was detected consisting of fine-mode and coarse-mode particles. At heights around 9 km a cirrus layer developed after 1500 UTC. Photometer measurements at cloud-free conditions became almost impossible after 1600 UTC.

Figure 9 shows the LIRIC products in terms of profiles of particle backscatter coefficient, extinction coefficient, and particle volume concentration for the fine-mode and the coarse-mode fraction. LIRIC calculations were performed with cloud-screened lidar signal profiles for the time period from 1435–1536 UTC on 19 April 2010. The considered photometric measurements were taken at 1449 UTC. Lidar signals were only used up to 8.25 km height (reference point) because of cirrus cloud evolution above this height. The minimum measurement height  $z_{N_0}$  was set to 600 m.

According to the volume concentration profiles in Figure 9, a strongly varying mixture of fine-mode and coarse-mode particles was observed throughout the troposphere. Cumulus cloud development at around 1345 UTC at 1 km height (see Figure 8) indicates high relative humidity of

990 >80% close to the top of the boundary layer. Thus particle<sub>1045</sub>  
 water–uptake effects must be taken into account in the data  
 interpretation. The relative humidity was about 60% in the  
 lofted layer from 1.5–2.8 km and less than 30% in the layer  
 above 3.5 km height around 15:00 UTC (Ansmann et al.,  
 995 2012). After 16:00 UTC, the relative humidity increased and<sub>1050</sub>  
 was high up to 2.8 km height.

The backscatter and extinction coefficients retrieved with  
 LIRIC show a pronounced, fine–mode–dominated wave-  
 length dependence from 1–2.2 km. Above 2 km the backscat-  
 1000 ter coefficients are nearly the same for all wavelengths,<sub>1055</sub>  
 caused by the dominating coarse–mode particle fraction. The  
 reversed backscatter wavelength spectrum at low heights (0–  
 1 km) is related to the presence of irregularly shaped volcanic  
 particles and the use of the spheroidal model to compute the  
 1005 extinction–to–backscatter ratios. <sub>1060</sub>

In a similar way as for the Saharan dust case, Figures 10  
 to 13 show the LIRIC results for this volcanic event in com-  
 parison with POLIPHON profiles and Raman lidar observa-  
 tions of optical properties of the particles. These compar-  
 1010 isons are much more difficult to interpret than it was the case<sub>1065</sub>  
 for the Saharan dust outbreak. Coarse–mode volcanic dust  
 particles were mixed with fine–mode sulfate particles. The  
 degree of mixing changed with height and strong gradients  
 in the aerosol concentrations were observed. In view of these  
 1015 complex, height–variable aerosol conditions, a detailed error<sub>1070</sub>  
 analysis (identification of specific uncertainty sources) is not  
 possible. The column–related, height–independent volume–  
 specific backscatter and extinction coefficients as derived  
 from the AERONET observations for the different aerosol  
 1020 types introduce uncertainties in the LIRIC as well as the<sub>1075</sub>  
 POLIPHON results.

As can be seen in Figure 10, the profiles of the parti-  
 cle backscatter coefficients do not agree well with the ones  
 directly determined from the Raman lidar observations at  
 1025 heights below 2 km. Part of the systematic deviations in<sub>1080</sub>  
 the lowermost 2 km may be caused by an erroneous cor-  
 rection of the overlap effect. The LIRIC backscatter coef-  
 ficients are based on the elastic backscatter signals and are  
 thus very sensitive to uncertainties in the overlap correction.  
 1030 The Raman lidar backscatter values in Figure 10 are calcu-<sub>1085</sub>  
 lated from signal ratios (ratio of elastic backscatter signal to  
 nitrogen Raman signal) so that the overlap effect (affecting  
 both signals in almost the same manner) widely cancels out.  
 As mentioned, the uncertainty in the overlap correction can  
 1035 cause uncertainties of about 25% in the backscatter coeffi-<sub>1090</sub>  
 cients for heights below 1.5 km height which then decrease  
 quickly with height.

The LIRIC and POLIPHON total backscatter coefficients  
 in the layers from 2–3 km and 4–5.5 km height agree well.  
 1040 The spherical particle volume fraction was about 15% after<sub>1095</sub>  
 AERONET, finally 16.8% in the LIRIC data set, and 55%  
 after POLIPHON. This means that the non–spherical parti-  
 cle fraction is much higher in the case of the LIRIC pro-  
 files compared to POLIPHON. As a consequence, the LIRIC

non–spherical particle backscatter coefficients are, on aver-  
 age, larger in Figure 10 (central panel). A pronounced over-  
 estimation occurs in the layer from 1–2 km height. Conse-  
 quently a strong underestimation is found in the case of the  
 backscatter profile for spherical particles.

The comparison of the LIRIC coarse–mode backscatter  
 profiles with the LIRIC non–spherical particle backscatter  
 profiles indicates that the coarse–mode values are dominated  
 by spherical particles in the lowermost 1 km of the atmo-  
 sphere. Also the fine–mode particles are obviously mostly  
 spherical.

As a direct consequence of the strong difference in the  
 sphericity values, considerable deviations between the LIRIC  
 and the POLIPHON mass concentrations are visible in  
 Figure 11. If we eliminate the particle density impact  
 ( $\rho_1 = 1.6 \text{ g/cm}^3$  for spherical particles and  $\rho_2 = 2.6 \text{ g/cm}^3$   
 for non–spherical particles) and show the volume concen-  
 tration profiles (the basic LIRIC product), the findings re-  
 main almost the same. Thus, a more basic comparison in  
 terms of volume concentrations is not needed here. As in  
 the case of the backscatter coefficients, the coarse–mode par-  
 ticle mass concentrations (LIRIC, POLIPHON) agree rea-  
 sonably well above 2 km height, and strongly deviate in the  
 layer from 1–2 km height. The POLIPHON spherical parti-  
 cle mass concentrations at heights below 2 km are almost  
 a factor of 4 larger than the LIRIC/AERONET values. The  
 comparison of LIRIC coarse–mode and fine–mode mass pro-  
 files with the LIRIC profiles for non–spherical and spherical  
 particles show that most of the non–spherical volcanic dust  
 particles in the 1–2 km layer belong to the fine–mode.

However, it must be kept in consideration in these  
 POLIPHON/LIRIC comparisons that also the POLIPHON  
 profiles are based on AERONET retrieval products (see  
 Sect. 3.2) and are thus uncertain. Further assumptions and  
 related uncertainties affect the accuracy (Ansmann et al.,  
 2011a, 2012). The respective relative errors are in the range  
 from 20%–50%, as indicated in Figure 11. Furthermore, if  
 a part of the volcanic particles change from non–spherical  
 to spherical shape at high relative humidity, the fine–mode  
 mass concentration will be overestimated and the coarse–  
 mode mass concentration underestimated.

Figures 12 and 13 show the comparison of the LIRIC re-  
 sults with the direct Raman lidar observations of the 532 nm  
 lidar ratio, particle linear depolarization ratio, and several  
 Ångström exponents. Considering the complicated aerosol  
 situation with all the assumption uncertainties, the agreement  
 of the different lidar ratio profiles is reasonable. The differ-  
 ences between the depolarization ratios result from the as-  
 sumed sphericity of 16.8% (LIRIC) and derived sphericity  
 of 55% (POLIPHON).

The profiles of the Ångström exponents show partly strong  
 deviations, especially in the case of the backscatter and li-  
 dar ratio values. A negative Ångström exponent for the lidar  
 ratio, as observed with our Raman lidar, indicates an aged  
 aerosol with a high amount of comparably large fine–mode

particles (Müller et al., 2005; Nicolae et al., 2013). In such aerosol situations, the lidar ratio at 355 nm is significantly lower than the one at 532 nm. LIRIC retrieves the opposite, a positive lidar-ratio-related Ångström exponent. Such a complicated aerosol case can obviously not be adequately handled by the LIRIC/AERONET data analysis scheme. The found disagreement in the intensive aerosol parameters corroborate our statement at the beginning of this section that many basic assumptions of LIRIC are not valid under these conditions.

## 5 Conclusions

The LIRIC method was applied to two very different aerosol scenarios to evaluate the potential and limits of the retrieval of optical and microphysical properties of irregularly shaped dust particles. This new technique makes use of a combination of aerosol profile measurements with three-wavelength elastic-backscatter lidar and column-integrated aerosol observations with spectrally resolved sun-sky photometers.

Before the LIRIC analysis scheme can be applied, a careful overlap correction of the lidar signals is necessary, a reasonable assumption regarding the aerosol optical properties in the lowermost troposphere has to be made, and a careful Rayleigh backscattering and extinction computation based on actual temperature and pressure profiles has to be performed. It is essential that the entire troposphere is well covered by proper aerosol lidar observations. In general, the use of lidars with at least two receiver units for near-range and far-range observations is desirable to guarantee high-quality LIRIC products. Vice versa, small lidars such as ceilometers may cover the lowest heights only, but may not be able to provide proper aerosol observations in lofted layers in the middle and upper troposphere. LIRIC applications are difficult in these cases, too.

*A priori* AERONET retrieval products are required and can introduce significant uncertainties. The representation of irregularly shaped desert and volcanic dust particles by a size distribution of spheroidal particles is one important error source. The use of the same refractive-index characteristics for the fine and the coarse mode is another important source of uncertainty. In the case of complex aerosol layering and mixing the use of column-integrated (height-independent) AERONET parameters causes further uncertainties in the LIRIC products.

The LIRIC aerosol profiles were compared with results obtained with the single-wavelength polarization lidar method POLIPHON and direct Raman lidar observation of basic particle backscatter and extinction properties. Two cases were contrasted. A comparably simple, well stratified Saharan dust case in May 2008 with almost no spherical particles in the tropospheric column was discussed first. Then a rather complex case of layering of coarse volcanic dust and fine-mode anthropogenic and volcanic sulfate aerosol in April

2010 was presented. A detailed discussion of the findings and the potential impact of the assumed spheroidal particle model was possible for the Saharan dust outbreak, but not for the complex volcanic aerosol event.

In the Saharan dust case, typical uncertainty features (biases) for desert dust introduced by the use of the spheroidal particle model were found in the LIRIC-derived optical properties, similar to the ones observed during the SAMUM campaign in the AERONET data. However, coarse-mode particle mass concentrations obtained with LIRIC showed acceptable agreement with an alternative retrieval method which is not based on spheroidal particle assumptions. The reason is most probably that specific extinction coefficients are the basis in the mass concentration retrieval and extinction values are not very shape-sensitive.

In the complex volcanic aerosol case, also considerable deviations of the LIRIC-derived optical properties from the direct Raman lidar observations were found. Coarse-mode particle mass values also deviated from the ones obtained with the alternative POLIPHON technique. A detailed error analysis was not possible because of the very complex aerosol scenario and the large number of assumptions and critical LIRIC input parameters.

It is too early to draw general conclusions from the LIRIC studies done so far in the framework of EARLINET and ACTRIS activities. More scenarios with very different aerosol loadings, layering, and mixing including aerosol types from marine, over urban and biomass-burning aerosol to mineral and volcanic dust must be analyzed and discussed in order to further improve the synergistic lidar/photometer analysis techniques. Other particle shape models may be developed and tested to better reproduce the 180° scattering properties of irregularly shaped particles. Much more work of comparisons of LIRIC results, Raman lidar products, and also independent airborne *in situ* aerosol observations would be desirable. But *in situ* observations often suffer from inlet problems (cutoff prohibits that large particles are detected) and that particles are measured under dry rather than ambient humidity conditions.

Nevertheless, the presented two case studies demonstrate that LIRIC is a powerful and promising tool for the retrieval of optical and microphysical aerosol properties. As raw and ready-to-use elastic-backscatter lidar signals serve as input for the algorithm and photometric measurements are available through the AERONET website, an almost instantaneous and fast data analysis is possible. An automated version of LIRIC is currently under development.

*Acknowledgements.* The research leading to these results has been performed in the framework of ACTRIS Workpackage 20 (ACTRIS Joint Research Activity “Lidar and sun photometer”) and received funding from the European Union Seventh Framework Programme (FP7/2007–2013) under grant agreement n° 262254. Discussion within ACTRIS Workpackage 20 is gratefully acknowledged.

## References

- 1205 **References**
- Ansmann, A., Wandinger, U., Riebesell, M., Weitkamp, C., and Michaelis, W.: Independent measurement of extinction and backscatter profiles in cirrus clouds by using a combined Raman elastic-backscatter lidar, *Appl. Opt.*, 31, 7113–7131, 1992.
- 1210 Ansmann, A., Wagner, F., Müller, D., Althausen, D., Herber, A., von Hyoningen-Huene, W., and Wandinger, U.: European pollution outbreaks during ACE 2: Optical particle properties inferred from multiwavelength lidar and star-Sun photometry, *J. Geophys. Res.*, 107, D15, doi:10.1029/2001JD001109, 2002.
- 1215 Ansmann, A., Tesche, M., Seifert, P., Groß, S., Freudenthaler, V., Apituley, A., Wilson, K. M., Serikov, I., Linné, H., Heinold, B., Hiebsch, A., Schnell, F., Schmidt, J., Mattis, I., Wandinger, U., and Wiegner, M.: Ash and fine-mode particle mass profiles from EARLINET-AERONET observations over central Europe after the eruptions of the Eyjafjallajökull volcano in 2010, *J. Geophys. Res.*, 116, D00U02, doi:10.1029/2010JD015567, 2011a.
- 1220 Ansmann, A., Petzold, A., Kandler, K., Tegen, I., Wendisch, M., Müller, D., Weinzierl, B., Müller, T., and Heintzenberg, J.: Saharan Mineral Dust Experiment SAMUM-1 and SAMUM-2: what have we learned?, *Tellus, Ser. B*, 63, 403–429, doi:10.1111/j.1600-0889.2011.00555.x, 2011b.
- 1225 Ansmann, A., Seifert, P., Tesche, M., and Wandinger, U.: Profiling of fine and coarse particle mass: Case studies of Saharan dust and Eyjafjallajökull/Grimsvötn volcanic plumes, *Atmos. Chem. Phys.*, 12, 9399–9415, doi:10.5194/acp-12-9399-2012, 2012.
- 1230 Böckmann, C., Miranova, I., Müller, D., Scheidenbach, L., and Nessler, R.: Microphysical aerosol parameters from multiwavelength lidar, *J. Opt. Soc. Am. A*, 22, 518–528, 2005.
- 1235 Chaikovsky, A., Dubovik, O., Goloub, P., Balashevich, N., Lopatsin, A., Karol, Y., Denisov, S., and Lapyonok, T.: Software package for the retrieval of aerosol microphysical properties in the vertical column using combined lidar/photometer data (test version), Tech. rep., Institute of Physics, National Academy of Sciences of Belarus, Minsk, Belarus, 2008.
- 1240 Chaikovsky, A., Dubovik, O., Goloub, P., Tanré, D., Pappalardo, G., Wandinger, U., Chaikovskaya, L., Denisov, S., Grudo, Y., Lopatsin, A., Karol, Y., Lapyonok, T., Korol, M., Osipenko, F., Savitski, D., Slesar, A., Apituley, A., Arboledas, L. A., Biniotoglou, I., Kokkalis, P., Granados Muñoz, M. J., Papayannis, A., Perrone, M. R., Pietruczuk, A., Pisani, G., Rocadenbosch, F., Sicard, M., De Tomasi, F., Wagner, J., and Wang, X.: Algorithm and software for the retrieval of vertical aerosol properties using combined lidar/ radiometer data: Dissemination in EARLINET, in: *Proceedings of the 26th International Laser and Radar Conference*, vol. 1, Porto Heli, Greece, 25–29 June 2012, pp. 399–402, 2012.
- 1250 Dubovik, O.: Optimization of numerical inversion in photopolarimetric remote sensing, in: *Photopolarimetry in Remote Sensing*, edited by Videen, G., Yatskiv, Y., and Mishchenko, M., pp. 65–106, Kluwer Academic Publishers, Dordrecht, The Netherlands, 2004.
- 1255 Dubovik, O. and King, M. D.: A flexible inversion algorithm for retrieval of aerosol optical properties from Sun and sky radiance measurements, *J. Geophys. Res.*, 105, 20 673–20 696, 2000.
- 1260 Dubovik, O., Holben, B. N., Lapyonok, T., Sinyuk, A., Mishchenko, M. I., Yang, P., and Slutsker, I.: Non-spherical aerosol retrieval method employing light scattering by spheroids, *Geophys. Res. Letts.*, 29, 1415, doi:10.1029/2001GL014506, 2002.
- Dubovik, O., Sinyuk, A., Lapyonok, T., Holben, B. N., Mishchenko, M., Yang, P., Eck, T. F., Volten, H., Munoz, O., Wehlmann, B., van der Zande, W. J., Leon, J.-F., Sokorin, M., and Slutsker, I.: Application of spheroid models to account for aerosol particle nonsphericity in remote sensing of desert dust, *J. Geophys. Res.*, 11, D11208, doi:10.1029/2005JD006619, 2006.
- Eadie, W. T. D., Drijard, D., James, F. E., Roos, M., and Sadoulet, B.: *Statistical Methods in Experimental Physics*, North-Holland Publishing Company, Amsterdam, London, 1971.
- Gasteiger, J., Wiegner, M., Groß, S., Freudenthaler, V., Toledano, C., Tesche, M., and Kandler, K.: Modelling lidar-relevant optical properties of complex mineral dust aerosols, *Tellus, Ser. B*, 63, 725–741, doi:10.1111/j.1600-0889.2011.00559.x, 2011a.
- Holben, B. N., Eck, T. F., Slutsker, I., Tanré, D., Buis, J. P., Setzer, A., Vermote, E., Reagan, J. A., Kaufman, Y. J., Nakajima, T., Lavenu, F., Jankowiak, I., and Smirnov, A.: AERONET – A federated instrument network and data archive for aerosol characterization, *Remote Sens. Environ.*, 66, 1–16, 1998.
- Kaufman, Y., Tanré, D., Léon, J.-F., and Pelon, J.: Retrievals of profiles of fine and coarse aerosols using lidar and radiometric space measurements, *IEEE Transactions on Geoscience and Remote Sensing*, 41, 1743–1754, 2003a.
- Kaufman, Y. J., Haywood, J. M., Hobbs, P. V., Hart, W., Kleidman, R., and Schmid, B.: Remote sensing of vertical distributions of smoke aerosol off the coast of Africa, *Geophys. Res. Letts.*, 30, 1831, doi:10.1029/2003GL017068, 2003b.
- Latham, T. L., Kumar, P., Nenes, A., Dufek, J., Sokolik, I. N., Trail, M., and Russell, A.: Hygroscopic properties of volcanic ash, *Geophys. Res. Letts.*, 38, L11802, doi:10.1029/2011GL047298, 2011.
- Léon, J.-F., Tanré, D., Pelon, J., Kaufman, Y. J., Haywood, J. M., and Chatenet, B.: Profiling of a Saharan dust outbreak based on a synergy between active and passive remote sensing, *J. Geophys. Res.*, 108, 8575, doi:10.1029/2002JD002774, 2003.
- Lopatin, A., Dubovik, O., Chaikovsky, A., Goloub, P., Lapyonok, T., Tanré, D., and Litvinov, P.: Enhancement of aerosol characterization using synergy of lidar and sun-photometer coincident observations: the GARRLiC algorithm, *Atmospheric Measurement Techniques Discussions*, 6, 2253–2325, doi:10.5194/amtd-6-2253-2013, <http://www.atmos-meas-tech-discuss.net/6/2253/2013/>, 2013.
- Mattis, I., Ansmann, A., Müller, D., Wandinger, U., and Althausen, D.: Multiyear aerosol observations with dual-wavelength Raman lidar in the framework of EARLINET, *J. Geophys. Res.*, 109, D13203, doi:10.1029/2004JD004600, 2004.
- Müller, D., Wandinger, U., and Ansmann, A.: Microphysical particle parameters from extinction and backscatter lidar data by inversion with regularization: Theory, *Appl. Opt.*, 38, 2346–2357, 1999.
- Müller, D., Mattis, I., Wandinger, U., Ansmann, A., Althausen, D., and Stohl, A.: Raman lidar observations of aged Siberian and Canadian forest fire smoke in the free troposphere over Germany in 2003: Microphysical particle characterization, *J. Geophys. Res.*, 110, D17201, doi:10.1029/2004JD005756, 2005.
- Müller, D., Ansmann, A., Mattis, I., Tesche, M., Wandinger, U., Althausen, D., and Pisani, G.: Aerosol-type-dependent lidar ratios observed with Raman lidar, *J. Geophys. Res.*, 112, D16202,

- doi:10.1029/2006JD008292, 2007.
- Müller, D., Ansmann, A., Freudenthaler, V., Kandler, K., Toledano, C., Hiebsch, A., Gasteiger, J., Esselborn, M., Tesche, M., Heese, B., Althausen, D., Weinzierl, B., Petzold, A., and von Hoyer, W.: Mineral dust observed with AERONET Sun photometer, Raman lidar and in situ instruments during SAMUM 2006: Shape-dependent particle properties, *J. Geophys. Res.*, 115, D11207, doi:10.1029/2009JD012523, 2010b.
- Müller, D., Lee, K.-H., Gasteiger, J., Tesche, M., Weinzierl, B., Kandler, K., Müller, T., Toledano, C., Otto, S., Althausen, D., and Ansmann, A.: Comparison of optical and microphysical properties of pure Saharan mineral dust observed with AERONET Sun photometer, Raman lidar, and in situ instruments during SAMUM 2006, *J. Geophys. Res.*, 117, D07211, doi:10.1029/2011JD016825, 2012.
- Müller, D., Veselovskii, I., Kolgotin, A., Tesche, M., Ansmann, A., and Dubovik, O.: Vertical profiles of pure dust and mixed smoke–dust plumes inferred from inversion of multiwavelength Raman/polarization lidar data and comparison to AERONET retrievals and in situ observations, *Appl. Opt.*, 52, 3178–3202, 2013.
- Nicolae, D., Nemuc, A., Müller, D., Talianu, C., Vasilescu, J., Belegante, L., and Kolgotin, A.: Characterization of fresh and aged biomass burning events using multiwavelength Raman lidar and mass spectrometry, *J. Geophys. Res.*, 118, doi:10.1002/jgrd.50324, 2013.
- O’Neill, N. T., Eck, T. F., Smirnov, A., Holben, B. N., and Thulasiraman, S.: Spectral discrimination of coarse and fine mode optical depth, *J. Geophys. Res.*, 108, 4559, doi:10.1029/2002JD002975, 2003.
- Schumann, U., Weinzierl, B., Reitebuch, O., Schlager, H., Minikin, A., Forster, C., Baumann, R., Sailer, T., Graf, K., Mannstein, H., Voigt, C., Rahm, S., Simmet, R., Scheibe, M., Lichtenstern, M., Stock, P., Rüba, H., Schäuble, D., Tafferner, A., Rautenhaus, M., Gerz, T., Ziereis, H., Krautstrunk, M., Mallaun, C., Gayet, J.-F., Lieke, K., Kandler, K., Ebert, M., Weinbruch, S., Stohl, A., Gasteiger, J., Groß, S., Freudenthaler, V., Wiegner, M., Ansmann, A., Tesche, M., Olafsson, H., and Sturm, K.: Airborne observations of the Eyjafjalla volcano ash cloud over Europe during air space closure in April and May 2010, *Atmos. Chem. Phys.*, 11, 2245–2279, doi:10.5194/acp-11-2245-2011, 2011.
- Schuster, G. L., Vaughan, M., MacDonnell, D., Su, W., Winker, D., Dubovik, O., Lapyonok, T., and Trepte, C.: Comparison of CALIPSO aerosol optical depth retrievals to AERONET measurements, and a climatology for the lidar ratio of dust, *Atmos. Chem. Phys.*, 12, 7431–7452, doi:10.5194/acp-12-7431-2012, 2012.
- Sugimoto, N., Uno, I., Nishikawa, M., Shimizu, A., Matsui, I., Dong, X., Chen, Y., and Quan, H.: Record heavy Asian dust in Beijing in 2002: Observations and model analysis of recent events, *Geophys. Res. Letts.*, 30, 1640, doi:10.1029/2002GL016349, 2003.
- Tesche, M., Ansmann, A., Müller, D., Althausen, D., Engelmann, R., Freudenthaler, V., and Groß, S.: Separation of dust and smoke profiles over Cape Verde by using multiwavelength Raman and polarization lidars during SAMUM 2008, *J. Geophys. Res.*, 114, D13202, doi:10.1029/2009JD011862, 2009a.
- Tesche, M., Ansmann, A., Müller, D., Althausen, D., Mattis, I., Heese, B., Freudenthaler, V., Wiegner, M., Esselborn, M., Pisani, G., and Knippertz, P.: Vertical profiling of Saharan dust with Raman lidars and airborne HSRL in southern Morocco during SAMUM, *Tellus, Ser. B*, 61, 144–164, 2009b.
- Veselovskii, I., Kolgotin, A., Griaznov, V., Müller, D., Wandinger, U., and Whiteman, D. N.: Inversion with regularization for the retrieval of tropospheric aerosol parameters from multiwavelength lidar sounding, *Appl. Opt.*, 41, 3685–3699, 2002.
- Veselovskii, I., Dubovik, O., Kolgotin, A., Lapyonok, T., Girolamo, P. D., Summa, D., Whiteman, D. N., Mishchenko, M., and Tanré, D.: Application of randomly oriented spheroids for retrieval of dust particle parameters from multiwavelength lidar measurements, *J. Geophys. Res.*, 115, D21203, doi:10.1029/2010JD014139, 2010.
- Volten, H., Munoz, O., Rol, E., deHaan, J. F., and J. W. Hovenier, W. V., Muinonen, K., and Nousiainen, T.: Scattering matrices of mineral aerosol particles at 441.6 nm and 632.8 nm, *J. Geophys. Res.*, 106, doi:10.1029/2001JD900068, 2001.
- Wagner, J.: Microphysical properties retrieved from combined lidar sun photometer measurements, University Master Thesis, Universität Leipzig, Germany, Sächsische Landesbibliothek — Staats- und Universitätsbibliothek Dresden, available at: <http://nbn-resolving.de/urn:nbn:de:bsz:15-qucosa-99830>, 2012.
- Wandinger, U. and Ansmann, A.: Experimental determination of the lidar overlap profile with Raman lidar, *Appl. Opt.*, 41, 511–514, 2002.

**Table 1.** Atmospheric and lidar input parameters and assumptions in the LIRIC and POLIPHON mass concentration retrievals as used in the paper. Overlap correction has only an impact on POLIPHON results for heights below about 2500 m.

Input parameter	LIRIC	POLIPHON
Overlap correction	×	(×)
Minimum/Maximum heights	×	
Rayleigh scattering, actual atmospheric profile	×	×
Reference backscatter coefficient	×	×
Refractive index, height-independent, same for fine and coarse mode	×	×
Column-mean sphericity, same for fine and coarse mode	×	×
Ratio of fine-mode spherical to non-spherical particles, height-independent	×	
Particle size distribution, height-independent	×	×
Spheroidal particle model (in $b_{m,s}(\lambda)$ computation)	×	
Volume-specific backscatter coefficient $b_{m,s}(\lambda)$ , height-independent	×	
Spheroidal particle model (in $a_{m,s}(\lambda)$ computation)	×	×
Volume-specific extinction coefficient $a_{m,s}(\lambda)$ , height-independent	×	×
Particle densities, fine mode, coarse mode $\rho_1, \rho_2$	×	×
Particle lidar ratio, fine mode, coarse mode		×
Fine-mode particles = spherical particles only		×
Coarse-mode particles = non-spherical particles only		×

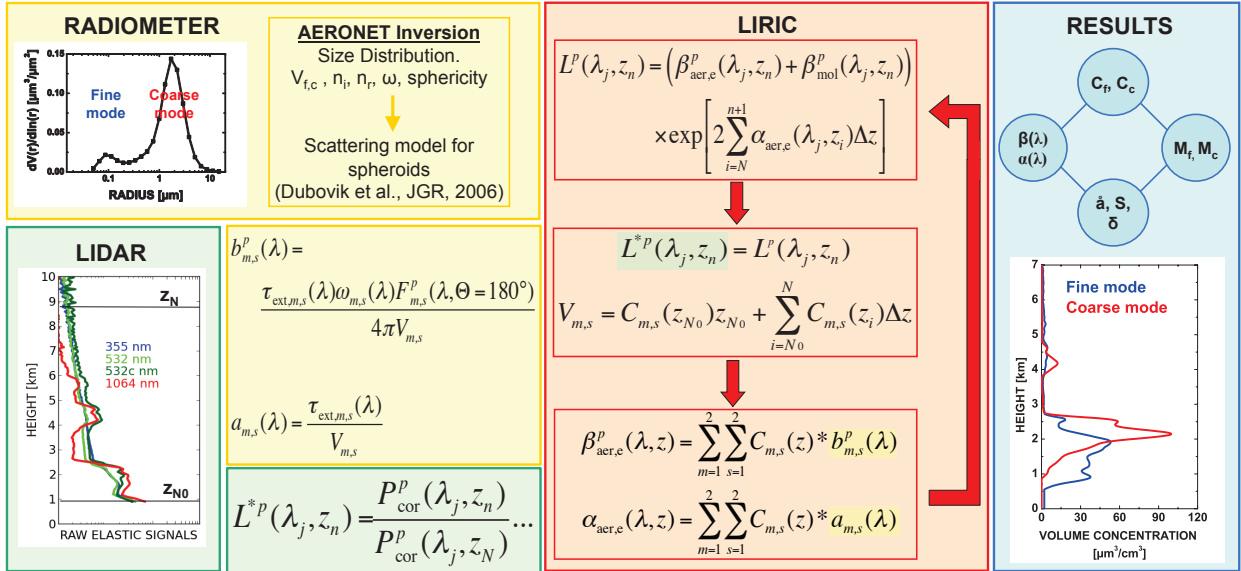


**Fig. 1.** Basic structure of LIRIC. Photometric information (radiometer, top yellow box) is used to retrieve height-independent (column) volume-specific backscatter and extinction coefficients  $b_{m,s}$  and  $a_{m,s}$  (center yellow box) for spherical ( $s = 1$ ) and non-spherical particles ( $s = 2$ ) of the fine mode ( $m = f$ ) and coarse mode ( $m = c$ ). A lidar signal term  $L$  (orange box, top) can be calculated with LIRIC by using profiles of backscatter and extinction coefficients (orange box, bottom) which, in turn, are calculated from the volume-specific coefficients  $b_{m,s}$  and  $a_{m,s}$  and profiles of particle volume concentration  $C_{m,s}(z)$ . Deviations between the observed lidar signal term  $L^*$  (green box) and the LIRIC expression  $L$  are minimized in order to retrieve optimized  $C_{m,s}(z)$  profiles (orange box, center). As a constraint, the integrals of the  $C_{m,s}(z)$  profiles must match the respective column values  $V_{m,s}$  as observed with AERONET photometer (orange box, center). LIRIC products (blue box) are profiles of particle optical properties (e.g., backscatter and extinction profiles, Ångström exponents, lidar and depolarization ratios) and microphysical properties (e.g., volume concentrations  $C_f$  and  $C_c$  as shown as profiles). The mass concentrations  $M_f$  and  $M_c$  for fine and coarse mode, respectively, are not LIRIC products.

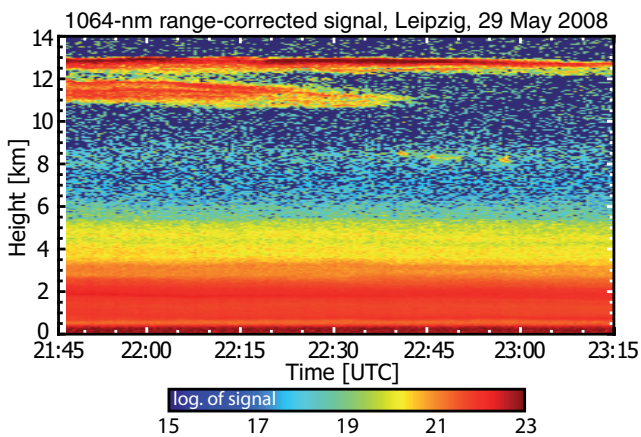


**Fig. 2.** Range-corrected signal at 1064 nm measured on 29 May 2008, 2147–2315 UTC (signal counts in logarithmic scale). The vertical resolution of the lidar measurement is 60 m, the temporal resolution is 30 s. The 500 nm AOT was 0.7–0.75 up to 6 km height in the evening of 29 May.

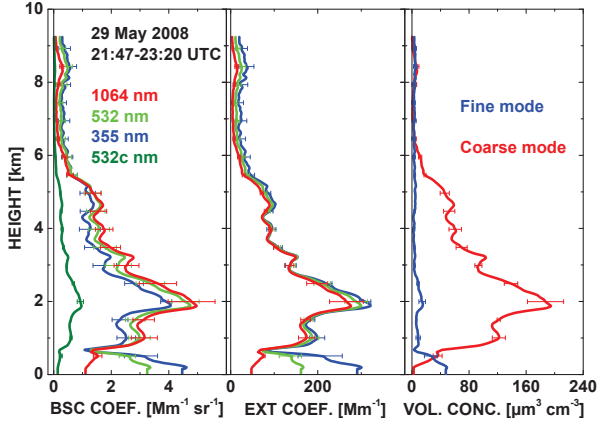


**Fig. 3.** Mean particle optical parameters (left: backscatter coefficient, center: extinction coefficient) for three laser wavelengths, backscatter coefficient for the cross-polarized 532 nm lidar channel (left, 532c nm, dark green), and particle volume concentration profiles (right) for fine-mode and coarse-mode fractions retrieved with the LIRIC method based on the lidar observations on 29 May 2008 shown in Figure 2. The vertical resolution is 15 m. The reference height is set to  $z_N = 9$  km and the minimum measurement height is  $z_{N_0} = 150$  m. The error bars show the uncertainties (standard deviation) of the LIRIC results (see discussion in section 3.1).

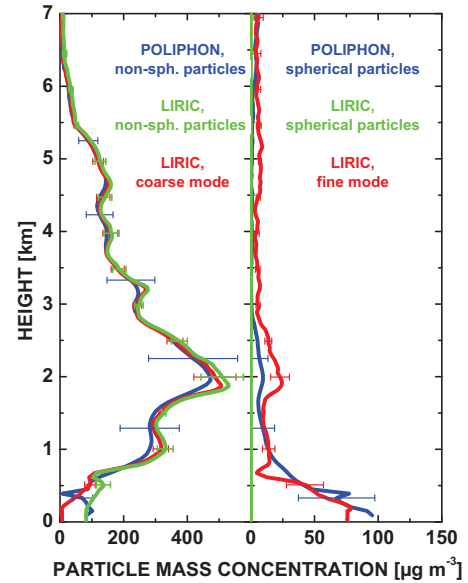


**Fig. 5.** Comparison of LIRIC- and POLIPHON-derived particle mass concentrations, observed on 29 May 2008. The blue POLIPHON curves are taken from Figure 2 of Ansmann et al. (2012). Error bars indicate the uncertainties (one standard deviation).

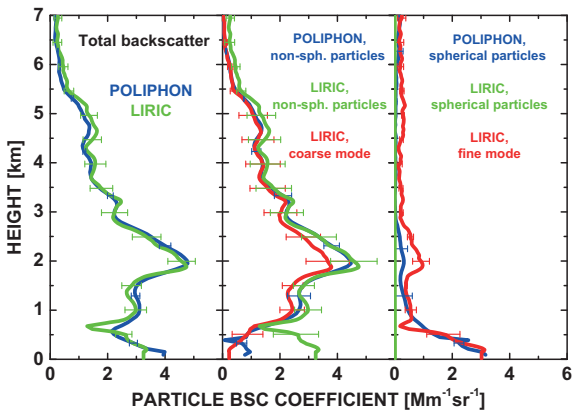


**Fig. 4.** Comparison of LIRIC- and POLIPHON-derived particle backscatter coefficients observed on 29 May 2008. The blue POLIPHON curves are taken from Figure 2 of Ansmann et al. (2012). The error bars indicate the uncertainties of the retrieval products as discussed in Sect. 3.1 (LIRIC) and in Ansmann et al. (2011a, 2012) (POLIPHON).

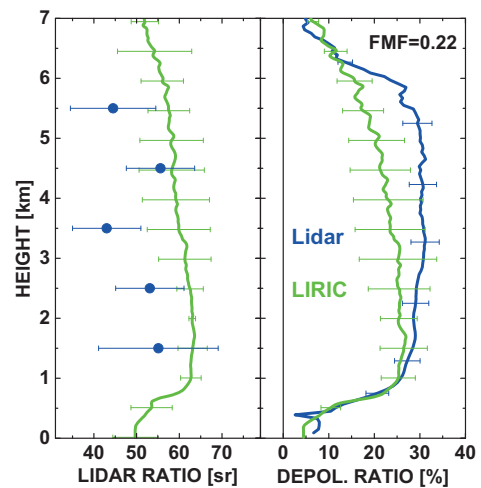


**Fig. 6.** Particle lidar ratio at 532 nm (blue circles) and particle depolarization ratio at 532 nm (blue curve) observed on 29 May 2008 with Raman lidar and derived by using the LIRIC profiles in Figure 3 (green curves). Raman lidar signals are smoothed with window lengths of about 1000 m in the case of the lidar ratio (blue symbols). Error bars indicate the uncertainties (one standard deviation). The depolarization ratio profile is given with 60 m resolution.

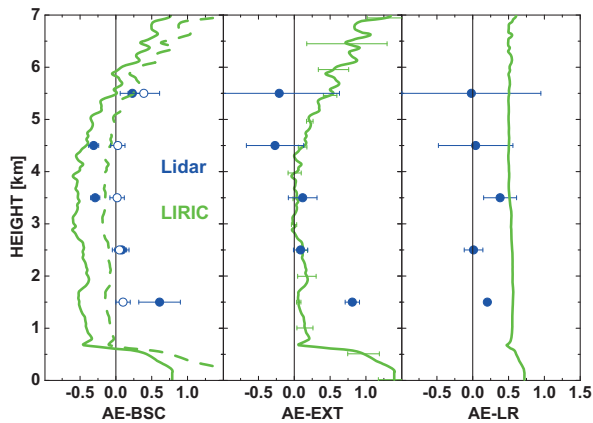


**Fig. 7.** Backscatter-related Ångström exponent (AE-BSC), extinction-related Ångström exponent (AE-EXT), and lidar-ratio-related Ångström exponent (AE-LR) observed on 29 May 2008 with Raman lidar (blue circles) and derived by using the LIRIC profiles in Figure 3 (green curves). Solid green curve and closed blue symbols show the Ångström exponents for the 355–532 nm wavelength range, dashed green curve and open blue symbols for the 532–1064 nm spectral range. As outlined by Ansmann et al. (2002),  $AE-EXT = AE-BSC + AE-LR$ . Raman lidar signals are smoothed with window lengths of about 1000 m in the case of extinction coefficients and the lidar ratio, and 60 m in the case of the backscatter coefficients. Errors bars indicate the uncertainties (one standard deviation). LIRIC error bars are given for AE-EXT only.

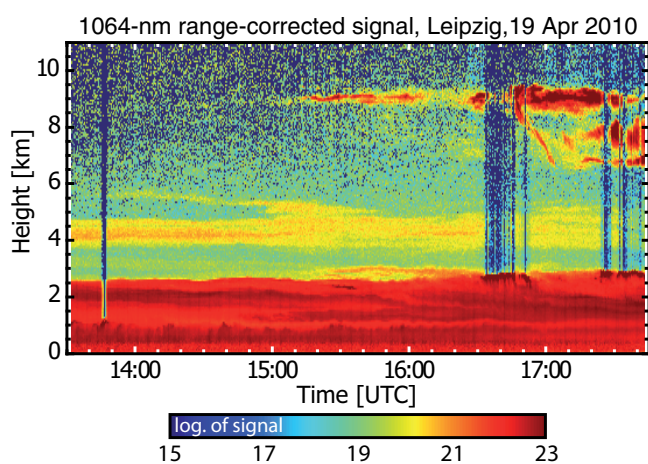


**Fig. 8.** Range-corrected signal at 1064 nm on 19 April 2010, 1332–1743 UTC. The vertical resolution is 60 m, the temporal resolution is 30 s. The 500 nm AOT was 0.7 up to 6 km height in the afternoon of 19 April.

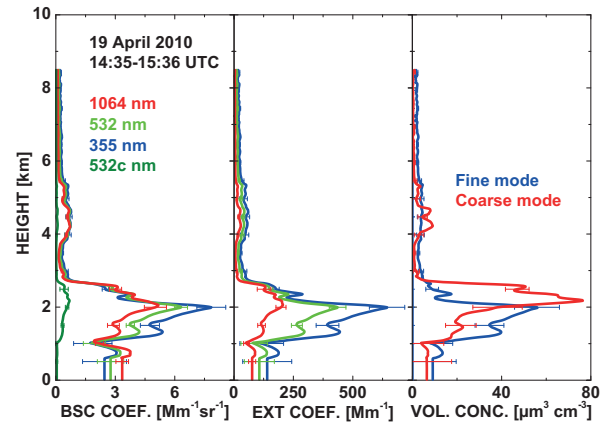


**Fig. 9.** Same as Figure 3, except for a volcanic dust observation on 19 April 2010, 1435–1536 UTC with retrieval reference height of  $z_N = 8.25$  km and minimum measurement height of  $z_{N_0} = 600$  m.

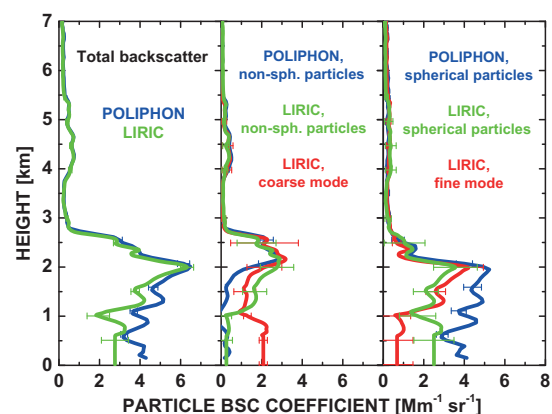


**Fig. 10.** Same as Figure 4, except for a volcanic dust observation on 19 April 2010. The POLIPHON curves are taken from Figure 4 of Ansmann et al. (2012).

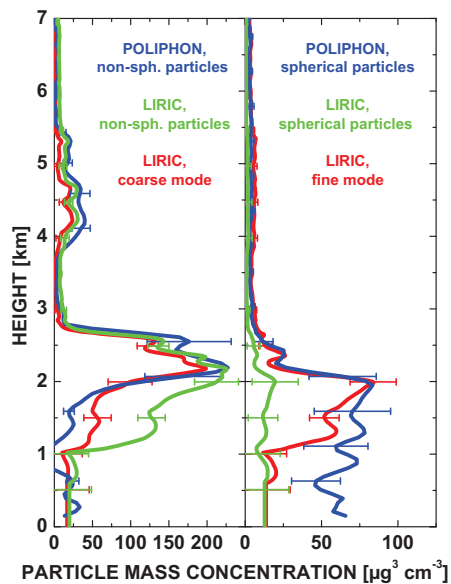


**Fig. 11.** Same as Figure 5, except for a volcanic dust observation on 19 April 2010. The POLIPHON curves are taken from Figure 4 of Ansmann et al. (2012).

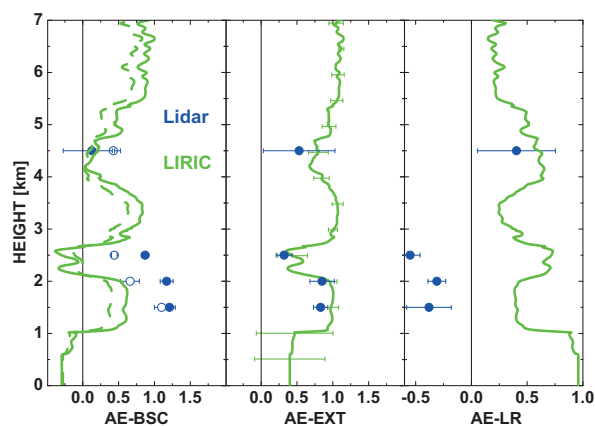


**Fig. 13.** Same as Figure 7, except for a volcanic dust observation on 19 April 2010. LIRIC profiles are derived from Figure 9 (green curves). Raman lidar observations (blue circles) were performed from 1330–1530 UTC. Raman lidar signals are smoothed with window lengths of 660 m in the case of extinction coefficients and the lidar ratio.

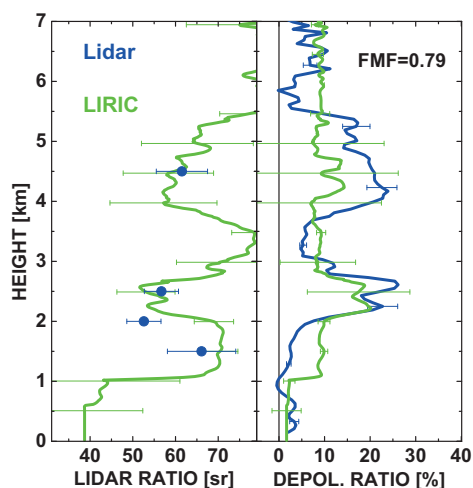


**Fig. 12.** Same as Figure 6, except for a volcanic dust observation on 19 April 2010, 1330–1530 UTC. Lidar signals are smoothed with 660 m vertical window length in the case of the Raman lidar solutions for the lidar ratio.